Allochthonous salt, structure and stratigraphy of the north-eastern Gulf of Mexico. Part II: Structure

Shengyu Wu, Albert W. Bally, Carlos Cramez
Department of Geology and Geophysics, Rice University, PO Box 1892, Houston, TX 77251, USA

Received 16 March 1990; revised 3 July 1990; accepted 9 July 1990

The kinematic evolution of allochthonous salt in the north-eastern Gulf of Mexico proceeds in three stages. (1) Since its middle Jurassic deposition, the Louann Salt was loaded by sediments causing episodic basinward movement of salt, ultimately leading to large concentrations of salt masses in a slope environment by the end of the Lower Cretaceous. (2) A regime of starved sedimentation during Late Cretaceous and Early Oligocene is responsible for the stabilization of these early salt accumulations. (3) With renewed rapid accumulation of sediments, during the Neogene and Pliocene, extensive allochthonous salt tongues and sheets formed by gravity spreading within the younger sediments of the slope. Autochthonous salt, allochthonous salt and detached allochthonous salt are typical stages of evolution. Major down to the basin growth faults separate allochthonous salt sheets from their original feeder stocks. Extension along down to the basin master growth faults is compensated mainly by salt withdrawal and partly by basinward shortening.

Keywords: north-eastern Gulf of Mexico; stratigraphy; allochthonous salt

Introduction

Middle Jurassic salt of the Gulf of Mexico basin controls structural styles, sedimentation, facies distribution and hydrocarbon accumulations. Various salt-related structures, such as salt rollers, salt pillows, diapiric salt stocks and walls and extrusive salt glaciers have been described in nature and modelled in the laboratory (e.g. Barton, 1933; Nettleton, 1934, 1955; Trusheim, 1960; Sannemann, 1968; Bishop, 1978; Halbouty, 1979; Jackson and Talbot, 1986; Talbot and Jackson, 1987a,b). Tonguelike or sheetlike salt bodies tectonically emplaced at stratigraphic levels above the source layer, such that the salt overlies stratigraphically younger strata, are termed 'allochthonous' in this paper (detached allochthonous salt of Bally, 1981; allochthonous salt of Worrall and Snelson 1989; detached diapir and salt namakier of Jackson and Talbot, 1986; salt nappe of Talbot and Jackson, 1987b; salt sill of Nelson and Fairchild, 1989; personal communication, M.P.A. Jackson, 1990). All other salt structures are termed 'autochthonous' (e.g., salt roller, salt anticline, salt pillow, diapir and welt). Both autochthonous and allochthonous salt are documented on seismic data from our study area.

The timing of salt movements, the evolution of allochthonous salt and related structures are the problems addressed in this paper. The study area was chosen in the north-eastern Gulf of Mexico where Cenozoic sedimentation rates are relatively low when compared with the central Gulf of Mexico. A grid *(Figure 1)* of recent seismic profiles, well logs, velocities, palaeontological and lithological information form the database for this study. Approximately 6000 miles of seismic data as deep as 13 s are integrated into sequence stratigraphic and structural analyses.

Many workers (Lehner, 1969; Amery, 1969; Wilhelm and Ewing, 1972; Martin, 1978; Humphris, 1978; Buffler *et al.*, 1978; Buffler, 1983; Bally, 1981; Talbot and Jackson, 1987b; Jackson *et al.*, 1988; Worrall and Snelson, 1989; Nelson and Fairchild, 1989; West, 1989) have proposed models explaining the origin of salt structures seen beneath the Sigsbee Escarpment. Most of the earlier studies were located in the central Gulf of Mexico where deep salt structures are not readily seen on seismic data. This led to a variety of interpretations of the evolution of gigantic salt structures beneath the Sigsbee Escarpment.

This paper does not directly address the structural history of the Sigsbee Escarpment with its complex and often poor seismic image of deep structures. Instead, we will document a model which describes the evolutionary stages of allochthonous salt in the north-eastern Gulf of Mexico. The timing of this model is based on the sequence stratigraphic framework presented in Wu *et al.* (1990). Seismic examples showing each of the evolutionary stages from the study area demonstrate the processes involved in the history of the allochthonous salt sheets. Because of similarities in geological setting and geometry of allochthonous salt we think that the salt structures beneath the Sigsbee Escarpment have possibly gone through similar evolutionary stages.

Structural styles

The structural styles in the Gulf of Mexico are the

0264–8172/90/040334–37

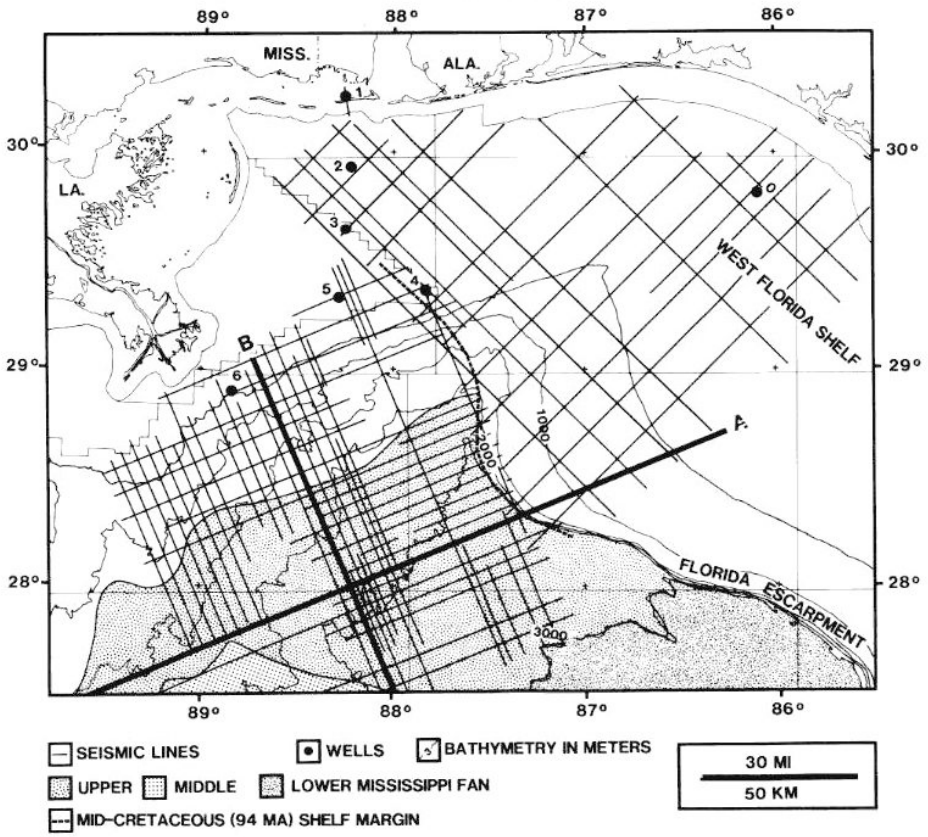

Figure 1 Index map of seismic lines and key well information used in this study. Locations of Line A *(Foldout 1)* and Line B *(Figure 3)* are shown on the map. Bathymetry from the Regional Map of Eastern Gulf of Mexico of NOAA, US Department of Commerce (1986). The Mississippi Fan is from Moore *et al.* (1978). The wells on the map are: 0-Sun No.1, Destin Dome block 166; 1-Mobil No.1, Mississippi Sound block 72; 2-Chevron No.1, Viosca Knoll block 30; 3-Shell No.1, Main Pass block 154; 4-Shell No.1, Main Pass block 253; 5-Chevron No. 2, Main Pass block 264; and 6-Exxon No. 1, Main Pass block 67

result of extensional and gravitational deformations. Gravity is the main driving force that formed most of the structures in the Gulf of Mexico. Three types of gravitational processes, i.e., gravity gliding, gravity spreading and diapirism (Ramberg, 1980) may be differentiated. As defined by Ramberg (1981, p.27), gravity gliding or gravity sliding is the down-slope sliding of rock masses. Gravity spreading or gravity collapse is defined as slow plastic vertical collapse and the complementary lateral spreading of rock masses. Gravitational diapirism is the gravitational re-adjustment of masses with an unstable distribution of density.

Widely distributed Mid-Jurassic Louann Salt (perhaps at least 2–3 km thick in the study area) is responsible for many post-salt structures in the Gulf of Mexico. Peripheral fault systems are associated with the up-dip depositional edge of Jurassic Louann Salt. Gravity gliding resulted in salt rollers that were dominantly formed in the Late Jurassic in areas of thin salt. Various diapiric and non-diapiric autochthonous salt structures such as salt anticlines, pillows, walls and stocks are dominant structural features in onshore salt basins and the De Soto Salt Basin. Spectacular allochthonous salt tongues and sheets are the most striking feature of the continental slope of the Gulf of Mexico. The Sigsbee escarpment is located at the basinward leading edge of these allochthonous salt sheets (Lehner, 1969; Amery, 1969, 1978; Antoine and Bryant, 1969; Wilhelm and Ewing, 1972; Humphris, 1978; Worrall and Snelson, 1989) as a result of active basinward gravity spreading of salt. To the north and behind the basinward spreading salt sheets are the well known Gulf Coast growth fault systems. Worrall and Snelson (1989) differentiate two different growth fault systems associated with salt: (1) the Texas Style with seaward dipping listric growth faults that are associated with very few shallow salt structures in offshore Texas; and (2) Louisiana style growth faults which are shorter, more arcuate, dip in various directions and are intimately associated with abundant salt domes offshore Louisiana. Overpressured shale is also associated with many structural features in the Gulf of Mexico.

Previous work on the Sigsbee Escarpment

The understanding of the structural complex associated with the Sigsbee Escarpment has evolved over an extended period through the efforts of many workers since the early 1950s. In the central Gulf of Mexico, the present seismic prospecting technology does not provide very good images for the deep structures. Further, the salt structures and the growth fault systems of the central Gulf of Mexico are in an advanced stage of development due to the enormous amount of the Cenozoic sediment influx. Thus direct evidence for the interpretations proposed by various workers is often incomplete for the deep structures of the continental slope, although excellent interpretations based on whatever data available have been made by many workers.

Pioneering work on the Sigsbee Escarpment began in

the early 1950s with refraction profiles and piston-coring (Ewing *et al.*, 1955). Shallow high velocity layers were found near the Sigsbee Scarp. Geophysical work in the Gulf of Mexico during the 1950s to early 1960s involving refraction (Antoine and Ewing, 1963), reflection (Ewing and Antoine, 1966), gravity (Talwani and Ewing, 1966) and magnetic measurements (Miller and Ewing, 1956), revealed that: (1) the Sigsbee Escarpment is not controlled by tectonic activity involving the basement; (2) the Sigsbee Escarpment is the front of a continuous belt of diapiric structures extending from the Texas–Louisiana coast to the scarp; (3) a seismic velocity of 4.4 km s^{-1} is associated with the shallow high velocity layer; and (4) a density of 2.15 g cm^{-3} is associated with the diapiric Sigsbee Knolls south of the scarp.

Work carried out by Shell in the late 1960s (Lehner, 1969; Wilhelm and Ewing, 1972) conclusively confirmed the salt–tectonic origin of the Sigsbee Escarpment as postulated by earlier workers. Shell, based on data from sparker seismic profiles, drilled and cored 10 salt structures north of the scarp. The main conclusions of Lehner (1969) were as follows: (1) The structural grain and the topography of the continental slope are controlled primarily by salt tectonics. (2) The top salt surface is easily identified on seismic and sparker records as a strong reflector or as an envelope of diffraction patterns. (3) Salt pillows and swells with diameters of 15–20 nautical miles (28–37 km) are typical for the continental slope. (4) Most salt structures on the continental slope form sea-knolls or sea-mounts with elevations of as much as 5000 ft. The tops of the salt pillows on the lower slope reach a common elevation and create a flat, terrace-like topography. (5) On the lower slope, broad sedimentary troughs appear to 'sink' into a large salt mass. The salt is displaced laterally under the differential load of overburden. (6) The Sigsbee scarp is the surface expression of a salt wall. (7) Active growth faults are observed along the shelf edge. These linear fault systems appear to be related to the flow of salt at depth away from the prograding shelf. (8) The slope salt is correlated tentatively with the Louann Salt at the northern rim of the Gulf basin and the evaporites in the Sigsbee Knolls. However, at this stage the salt structures beneath the Sigsbee Scarp were believed by Lehner (1969) to be the top of a large diapiric salt massif.

The salt–tectonic origin of the structures beneath the Sigsbee Escarpment was established during the late 1960s. In addition a seismic reflection survey across the continental slope and rise (de Jong, 1968) suggested the presence of a high velocity layer north of the Sigsbee Scarp. The high velocity layer was believed to be the top of the Louann Salt by de Jong (1968). The high velocity layer rests on a thick sequence of undisturbed strata of lower velocities. Amery (1969) interpreted a high velocity anomaly associated with the Sigsbee Escarpment to be salt extruded 10 km over flat-lying beds south of the scarp. The extrusion and the topographic form of the scarp are related by Amery to basinward flow of sediments and salt from under the thick shelf-slope sedimentary wedge. A study of Antoine and Bryant (1969) also suggested that salt migrated down-dip into the deeper parts of the basin as a result of overburden pressures. They suggested that in areas of carbonate build ups, competency of the carbonate material impeded formation of salt piercement structures; instead, horizontal migration of salt towards the deep basin seems to have taken place. Although down-dip salt movement is inferred beneath the Sigsbee Escarpment, the postulated lateral movement was very limited (Amery, 1978).

Large-scale down-slope salt movement was inferred by Wilhelm and Ewing (1972) and by Humphris (1978). Indeed over 100 km of basinward movement of salt mass was inferred by Humphris (1978). Based on previous work, Humphris (1978) suggested that the Sigsbee Escarpment is the surface expression of the leading edge of a probably Jurassic salt mass that extruded over Quaternary and Tertiary sediments. The work of Watkins *et al.* (1978) confirmed that salt extended for a large distance over younger sediments. Humphris (1978; following Wilhelm and Ewing, 1972) compared the lateral salt movement with the extrusive flow of ice in a glacier. Humphris (1978) suggested that the salt masses associated with the Sigsbee Escarpment are still connected with the original salt bed.

Regional multi-fold seismic data collected by the University of Texas from 1975 to 1978 provided more information about the structures associated with the Sigsbee Escarpment (Buffler *et al.*, 1978, Buffler 1983). Buffler (1983) also interpreted the Sigsbee Escarpment as the leading edge of a mobilized mass (possibly salt or a salt–sediment mixture). Their data show that to the east the Sigsbee scarp is buried by, and loses its bathymetric identity beneath, the huge Plio–Pleistocene Mississippi Fan.

A completely detached allochthonous nature of the salt masses associated with the Sigsbee Escarpment was proposed by Bally (1981). He suggested, based on a section across the Gulf of Mexico, that salt beneath the upper continental slope of the northern Gulf of Mexico is separated from the original depositional salt bed. Following the work of Humphris (1978), Buffler *et al.* (1978) and Watkins *et al.* (1978), he also suggested a large basinward salt movement towards the deep Gulf basin. Further up in the sequence and towards the Gulf of Mexico, extensive listric–normal growth faults dissect Tertiary clastics and flatten within the high pore pressure shale section at depth.

The centrifugal experiments of Talbot and Jackson (1987b) and Jackson *et al.* (1988) were attempted to model the Sigsbee salt nappe complex. Salt nappes similar to the Sigsbee complex were reproduced by imposing a pre-existing basement step. The Sigsbee uplift postulated by Lehner (1969) and Buffler (1984) was taken as the prototype for the basement step in the laboratory model. A cross-section across the central northern Gulf of Mexico shows the interpretation of the Sigsbee nappe complex by Jackson *et al.* (1988). Their studies concluded that the salt nappe is a recumbent salt wall the base of which is a thrust surface that truncates the younger sediments.

The recent synthesis of Worrall and Snelson (1989) related the salt structures to the Neogene growth fault systems of the Gulf of Mexico. Using computer-aided palinspastic reconstructions Worrall and Snelson (1989) demonstrated that both Texas style and Louisiana style growth fault systems are due to the basinward movement of salt associated with the growth fault systems. The different map patterns of the two types of fault systems according to these workers are due to different shapes of sediment loads (i.e. elongated

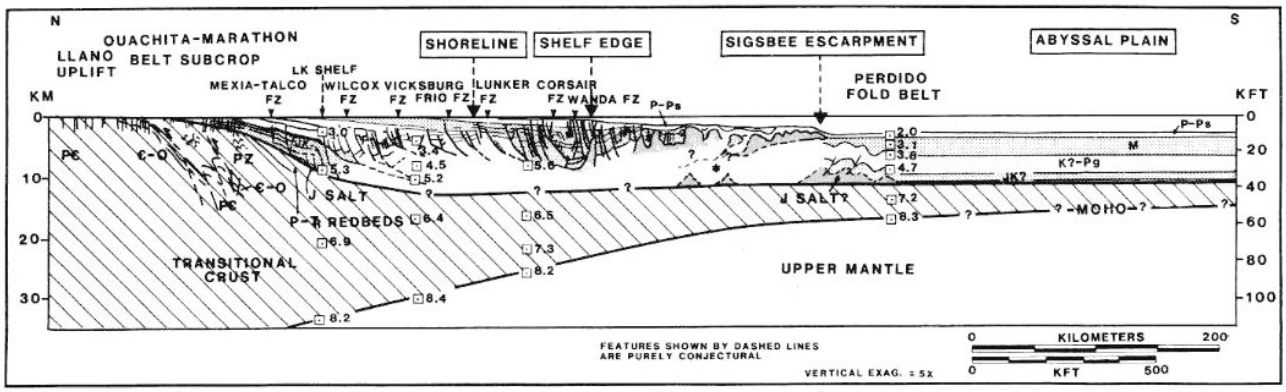

Figure 2 Interpretive summary cross-section of the Texas Gulf margin. Vertical exaggeration ×5. All dashed surfaces and salt features are highly conjectural and are not supported by seismic control. Asterisk (*) indicates that some shallow salt features may not root vertically to Jurassic salt level rather than laterally flowing masses; much uncertainty still exists for the deep structure of this area. (Redrawn after Worrall and Snelson, 1989).

intradeltaic loads *versus* circular deltaic loads). The cross-section of *Figure 2* shows their understanding of the structures of the northern Gulf of Mexico. A large allochthonous sheet is interpreted beneath and to the north of the Sigsbee Escarpment. The extensive growth fault systems to the north and behind the allochthonous salt are accommodated by the basinward flow of the allochthonous salt. Deep seismic profiles also revealed the Perdido fold belt with anticlines possibly cored by Jurassic Louann Salt welts (for definition of welt see Harrison and Bally, 1988), as illustrated in *Figure 2*. The folded belt is located basinward and beyond the Sigsbee Escarpment and below the allochthonous salt. This feature was not shown on any of the previous interpretations mentioned earlier.

Salt tectonics in the north-eastern Gulf of Mexico

Introduction

A regional seismic strike profile extending from the West Florida shelf to the slope area in the north-eastern Gulf of Mexico *(Foldout 1A-C)* best documents the structural styles of both autochthonous and allochthonous salt in the study area. The velocity effects are eliminated in a depth-converted section *(Foldout 1C)*. The base of the Jurassic Louann Salt can be interpreted on the seismic section. No major fault appears to separate the Florida shelf from the deep water Gulf of Mexico. A maximum of 4° of dip is observed on the base of Jurassic salt near Florida Escarpment *(Foldout 1C)*. The height of salt domes increases from the base of the Florida Escarpment in the east to the slope in the west. In a basinward direction non-diapiric salt pillows developed into diapiric domes. This progressive trend reflects the increase of the original salt thickness toward the basin. Thus younger, i.e. longer growing salt domes, correspond to thicker primary salt.

Minor extensional faults are observed in the Jurassic and Lower Cretaceous section at the Florida Escarpment. Some of the faults sole out within the autochthonous salt. Toward the deep Gulf, reverse faults suggest shortening. Again, reverse faults sole out within the autochthonous salt which forms a regional décollement level. Shortening ended during Middle–Upper Miocene. Shortening features disappear where autochthonous salt pinches out to the left.

A spectacular feature on this section *(Foldout 1)* is the allochthonous salt floating within the Miocene and Pliocene siliciclastic sediments. The larger allochthonous sheet is over 90 km wide and as much as 3 km thick. Overlying the allochthonous salt sheet is the structurally deformed Mississippi Fan. The intriguing salt sheets on this section serve as useful analogues for the understanding of the development of the Sigsbee Escarpment to the west, as they provide smaller scale models of similar features.

A seismic dip profile perpendicular to *Foldout 1* shows additional structural features associated with an allochthonous salt sheet *(Figure 3)*. On a much smaller scale the structural style of this profile is very similar to that of the regional profile across central Gulf of Mexico *(Figure 2;* Worrall and Snelson, 1989). The bathymetric expression of the frontal end of this allochthonous salt sheet is buried under the rapidly deposited Plio–Pleistocene sediments of the Mississippi Fan (Weimer, 1989). Autochthonous salt is concentrated at depth and below the middle slope of the Gulf and underlies the allochthonous salt sheets. A down to the basin master growth fault formed after the Mid-Cretaceous soles out within the Jurassic Louann Salt behind the allochthonous salt sheet. A complex system of minor normal faults dipping both seaward and landward soles out behind and on top of the allochthonous salt sheet. The top of the allochthonous salt sheet undulates as secondary domes develop. The allochthonous salt sheet truncates the sediments below and overthrusts the younger sediments. Deep shortening features occur basinward and below the frontal end of the allochthonous salt sheet. In the remainder of this paper each of the structural elements described here will be analysed in some detail using examples and semi-quantitative palinspastic reconstructions.

Depth conversions

Depth-converted sections in this study were made using an AIMS modelling program and Geoquest's interpretation workstation. Vertical rays are assumed for the ray tracing. Simplified gross velocities *(Table 1)* based on available check-shot velocities and published sources (Ewing *et al.*, 1960; Lehner, 1969; Amery, 1969) for each defined time interval are listed for the purpose of depth conversions used later in this study. Velocities are not accurate for each interval. As all the

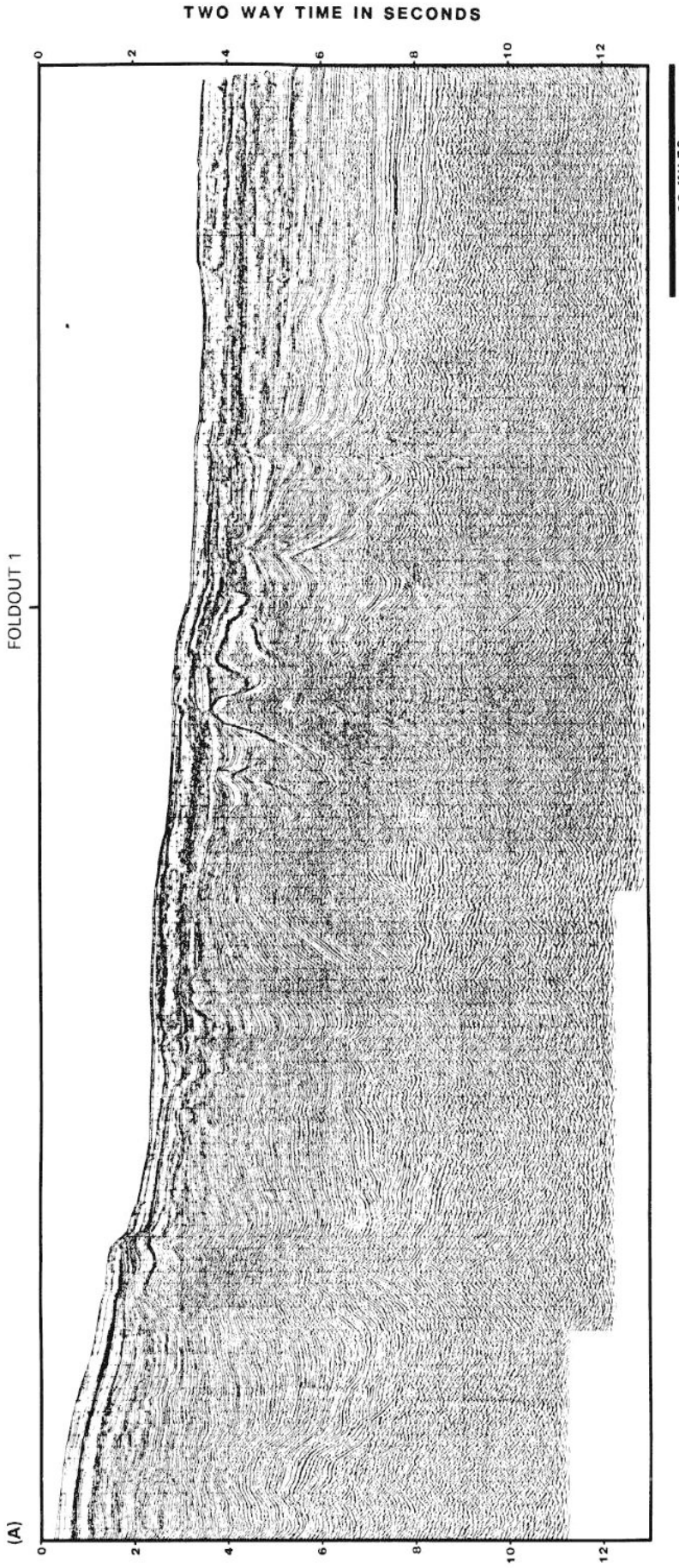

Figure 3 (A) Uninterpreted NW–SE structural dip seismic profile from north-eastern Gulf of Mexico (courtesy of GECO). For location see *Figure 1*. This intersects with the seismic line in *Foldout 1*. Part **(B)** is on the following page

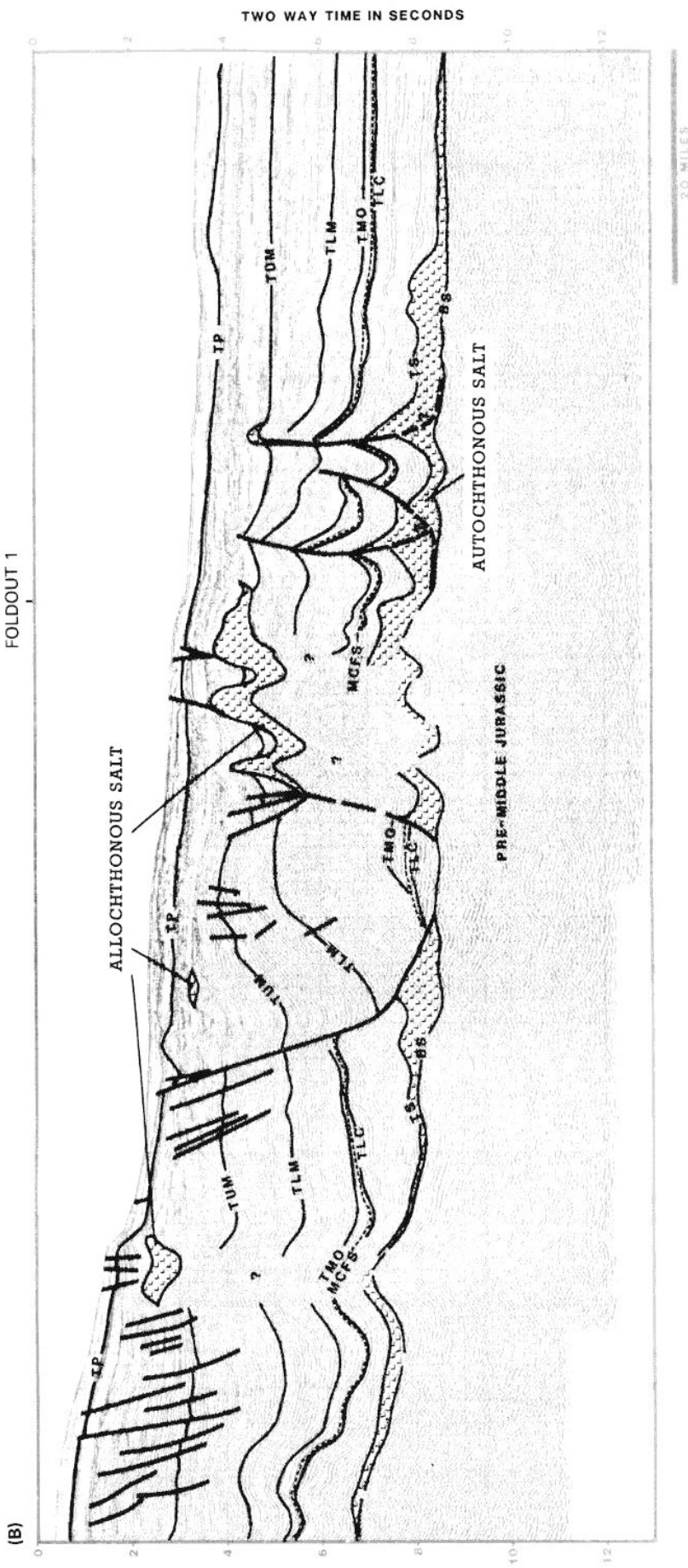

Figure 3 cont. **(B)** Interpreted seismic line in (A). BS, Base of Werner Anhydrite and Louann Salt, 158.5 Ma sequence boundary; TS, top of Louann Salt, 150.5 Ma sequence boundary; TJ, approximately top Jurassic, 128.5 Ma sequence boundary; TLC, top Lower Cretaceous, 94 Ma sequence boundary; MCFS, Middle Cretaceous Flooding Surface, 91.5 Ma maximum flooding surface; TMO, approximately top Middle Oligocene, 30 Ma sequence boundary; TLM, approximately top Lower Miocene, 15.5 Ma sequence boundary; TUM, approximately top Upper Miocene, 5.5 Ma sequence boundary; TP, approximately top Pliocene, 1.6 Ma sequence boundary. Area covered by L symbols is evaporite. Both autochthonous and allochthonous salt structures are shown

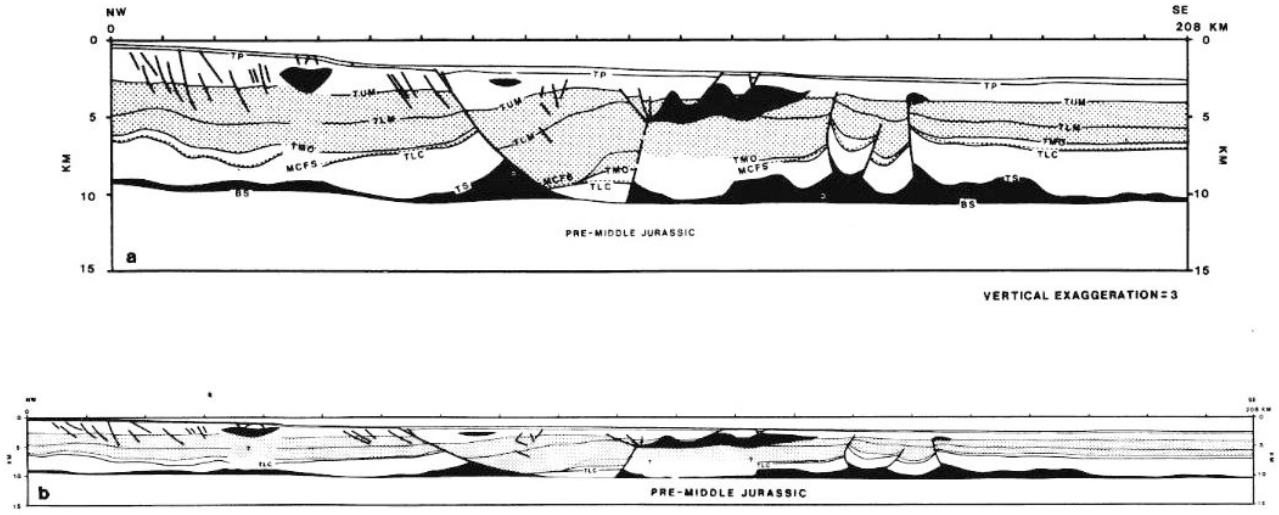

Figure 3 (C) Depth conversion of interpretation in (B). Both the vertically exaggerated and true-scale sections are shown in (a) and (b), respectively. Interval velocities for depth conversion are in *Table 1.*

Standard Chrono-Stratigraphy	Sequence Boundaries Name & Age	Interval Velocities Used in Depth Conversion (meters/second)		
(Ma)	(Ma)	Deep Water Area	Florida Terrace	Base of salt map
Sea water		1,500	1,500	1,500
Pleistocene		1,600		
1.65	(TP) 1.6			
Pliocene		2,000		
5.2	(TUM) 5.5			
Upper-Middle Miocene		2,500		
16.2	(TLM) 15.5		2,500	2,500
Lower Miocene-Upper Cretaceous		3,300		
	(TLC) 94			
96				
Lower Cretaceous-Upper Jurassic		4,600	4,300	
152	(TS) 150.5			4,500
Middle Jurassic Evaporite		4,500	4,500	
158.5	(BS) 158.5			
Pre-Middle Jurassic				

Table 1 Interval velocities for depth conversions. The interval velocities are constant for each time interval. This is a very approximate velocity structure based on the published velocities and the velocity surveys available to this study

velocity information available to this study is from the shelf and uppermost slope areas, it may differ from the velocities of the same stratigraphic interval in the slope area, especially when the lithology of the sediments is unknown and the depth changes. Nevertheless *Table 1* is probably good enough for the purpose of depth conversion in this study. The velocities used are adequate to eliminate the pull-up effects caused by the high velocity salt emplaced within the low velocity Late Tertiary sediments. A moderate smoothing of the depth-converted section and map is applied. The smoothed depth sections are converted back to two-way reflection time sections and used to constrain the final interpretations of seismic profiles.

Base and distribution of original autochthonous salt

The base of the autochthonous salt (BS or 158.5 Ma sequence boundary on interpreted seismic examples) is correlated throughout the study area. The base of the autochthonous salt is often recognized as the first flat-lying reflector which can be correlated below the acoustically opaque salt *(Foldout 1)*. The base of the salt is mapped and converted to depth in *Figure 4* using the interval velocities in *Table 1*. This is a contour map constructed by smoothing and interpolating the measurements at the locations where there are no overlying allochthonous salt tongues and sheets. The base of the autochthonous salt shows a regionally smooth surface gently dipping seaward. The maximum dip of the base salt is about 4° below the Florida Escarpment. Late Cenozoic–Pleistocene sediment loading is considered to be the principal cause of basement flexuring. There are no major faults separating the Florida Escarpment from the slope area at the base of autochthonous salt. This observation invalidates models for the opening of the Gulf of Mexico that involve major transform faults in the study

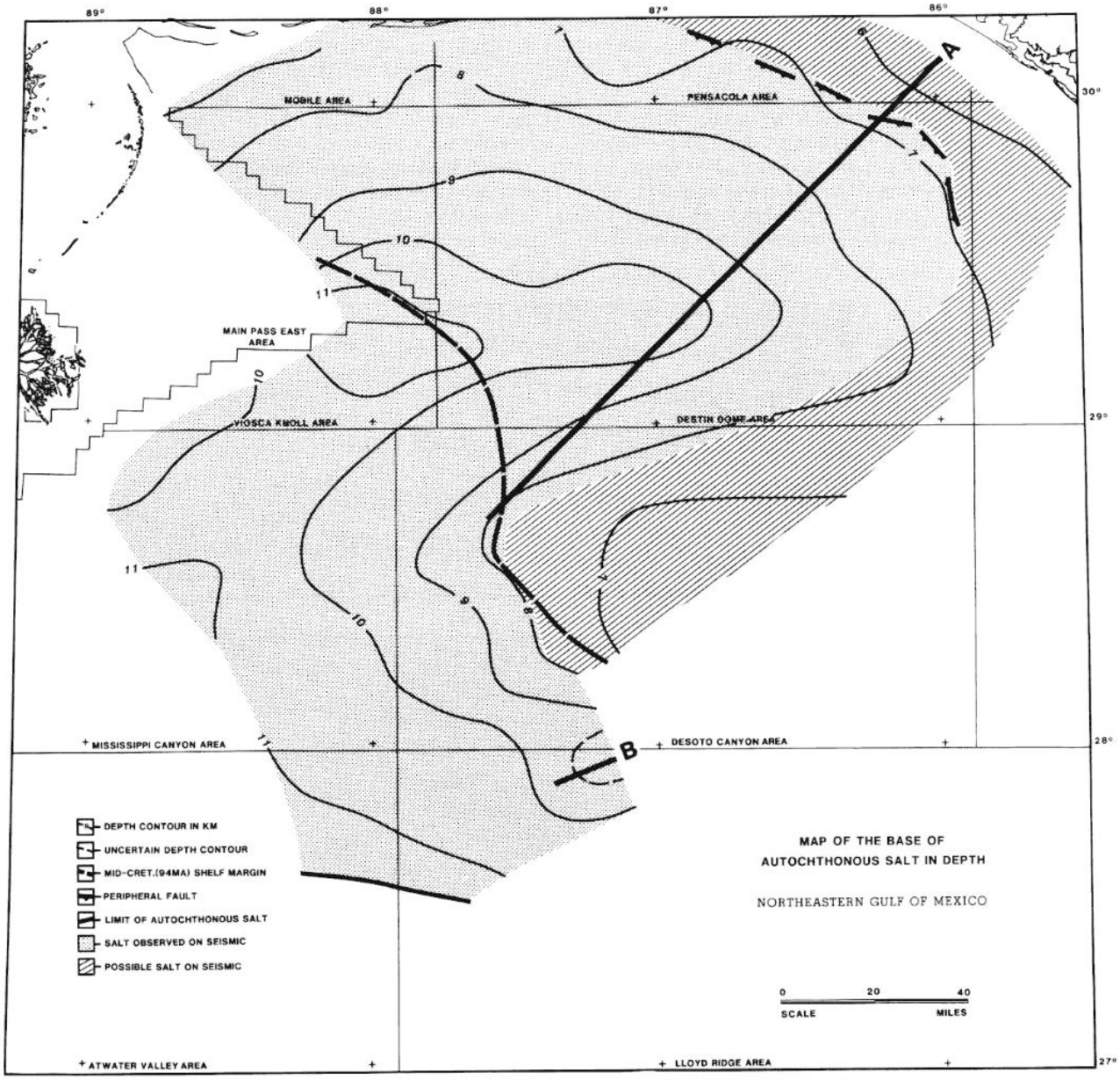

Figure 4 Depth map (in km) of the base of autochthonous salt in the north-eastern Gulf of Mexico. The interval velocities used in the depth conversion of the base of autochthonous salt are given in *Table 1*. Line A *(Foldout 2)* and Line B *(Figure 5)* are examples of the base of autochthonous salt. The rest of the base of autochthonous salt can be seen in the previous and following seismic profiles

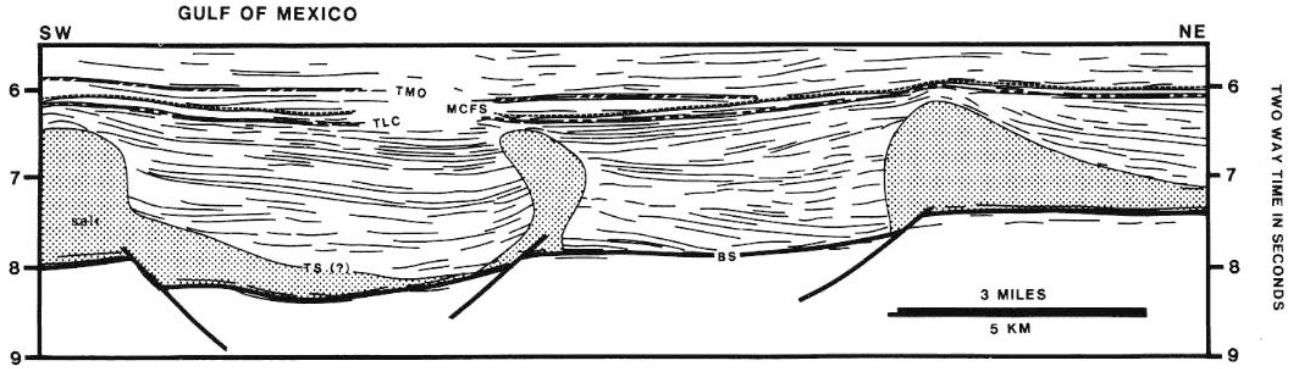

Figure 5 Line drawing of a seismic profile from slope study area. For location see *Figure 4.* The seismic profile shows the faulted base of autochthonous salt. This type of base of autochthonous salt is only observed in a small area around this example

area (Klitgord *et al.*, 1984).

Seismic data show that the base of autochthonous salt is a smooth surface in most of the study area where the base of the salt reflector is observed (see previous and following seismic examples). Two extreme examples of the base of the autochthonous salt are shown in *Foldout 2 and Figure 5.* As shown in the line drawing *(Foldout 2)* the base of autochthonous salt is a regional unconformity truncating underlying strata underneath the Middle Cretaceous shelf of the Destin Dome Area. In contrast, an exceptionally faulted base of autochthonous salt is observed in the line drawing of a seismic profile shown in *Figure 5* from the south-eastern corner of the study area basinward of the Florida Escarpment. However, the observed faulted base of autochthonous salt is located in a small area around the example *Figure 5.* Based on most of the data available, we assume that the base of the autochthonous salt beneath the allochthonous salt is a relatively smooth surface without major faults.

The original thickness of the Louann Salt is very difficult to estimate because salt has moved laterally and vertically since its Mid Jurassic (158.0–150.5 Ma) deposition. However, the semi-quantitative palinspastic reconstructions suggest that at least 2–3 km of salt was deposited in the slope area. The preserved autochthonous salt beneath the Middle Cretaceous shelf is relatively thin, except for the Destin Dome

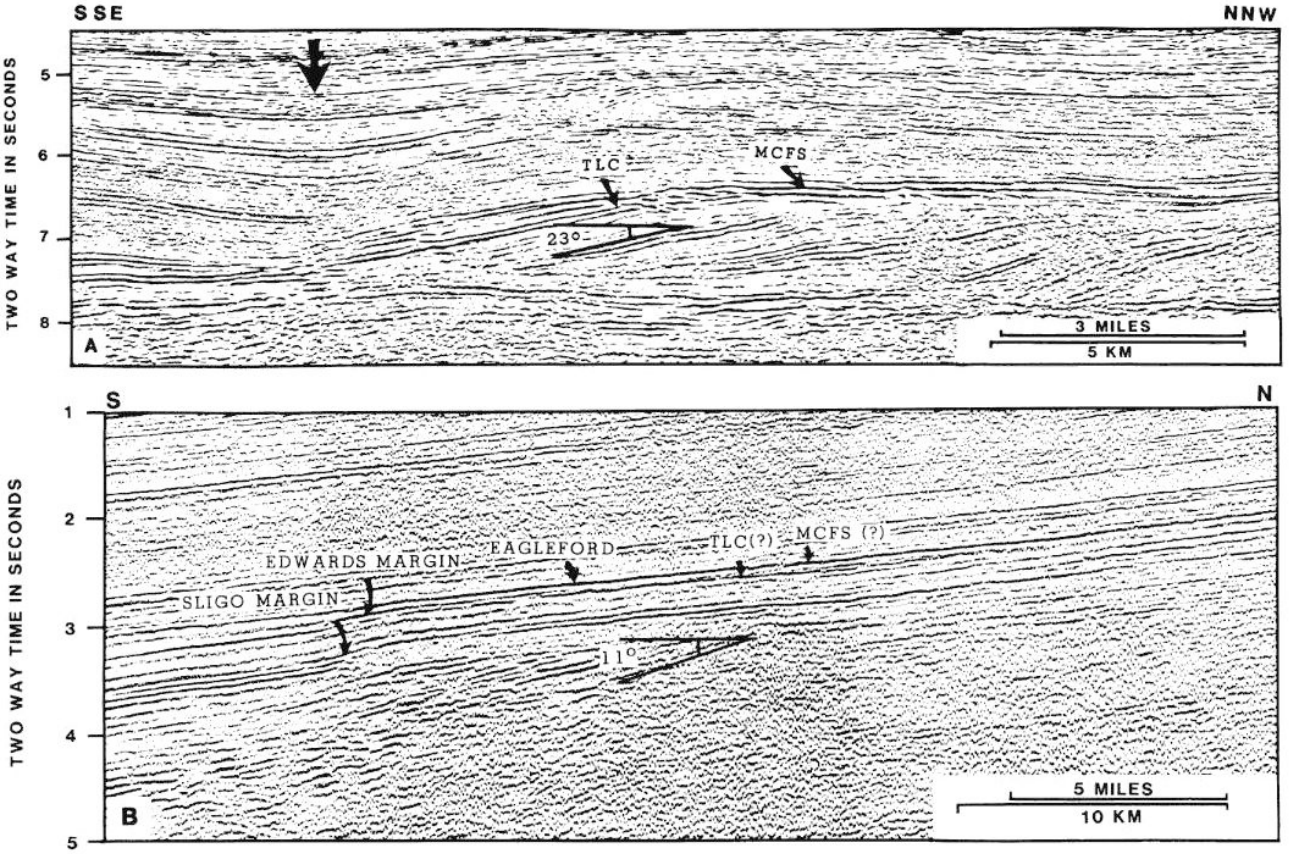

Figure 6 Comparison of part of the pseudo-clinoformal patterns and a seismic example of progradations of Lower Cretaceous carbonate platform margins from Vernon Parish, Louisiana. Note that (A) and (B) have different horizontal scales. Angles are true angles following depth conversions. The height of pseudo-clinoforms in (A) is greater than the height of the clinoforms in (B). **(A)** Portion of the pseudo-clinoformal patterns of *Foldout 3.* Note from the location of the seismic line in *Figure 11* that the example is basinward of the Middle Cretaceous shelf margin. **(B)** Example of the Lower Cretaceous carbonate platform margins (From Tyrrell, Jr. and Scott, 1988)

Area. Autochthonous salt generally thickens basinward and pinches out at its southern limit *(Foldout 1* and *Figure 4)*. Most of the preserved autochthonous salt may be concentrated below the allochthonous salt sheet and in the fold belt, i.e. a zone of folds and thrusts about 80 km wide in a north–south direction *(Figure 3)*. As will be shown, much of the formerly more landward salt has moved away from its original position during later deposition of the Meso–Cenozoic overburden.

Early salt-related deformations

A peripheral fault system associated with the up-dip limit of Jurassic salt is observed in the eastern end of the study area *(Figure 4 and Foldout 2)*. This fault system started during the deposition of Smackover carbonates and continued into the Cretaceous. The earliest deformation related to salt was triggered by the deposition of Smackover carbonates above Louann Salt. As a consequence of gravitational gliding on a gentle slope underlying the shallow water Smackover carbonates, the broken denser carbonate layers rotated on less dense salt. Salt rollers (Bally, 1981; Jackson and Talbot, 1986) thus formed. The formation of rollers dominated the structural deformation during the upper Jurassic deposition of carbonate–clastic rocks on the shelf *(Foldout 2; Foldouts 3* and *4* of Wu *et al.* (1990)). The gravity instability due to the presence of dip combined with a density inversion initiated the withdrawal of salt in the down-dip direction and the rotation of carbonate blocks along a down-slope direction. These structures are inferred to have formed in shallow water because the tops of the carbonate blocks were truncated by regional unconformities (Bally, 1981; *Foldouts 1, 3* and *4* of Wu *et al.* (1990)).

Middle Cretaceous concentration and stabilization of salt

Our seismic data suggest various periods of down-dip salt movements due to up-slope sediment loading that occurred since the deposition of Mid-Jurassic salt. A series of 'pseudo-clinoformal' stratal patterns are

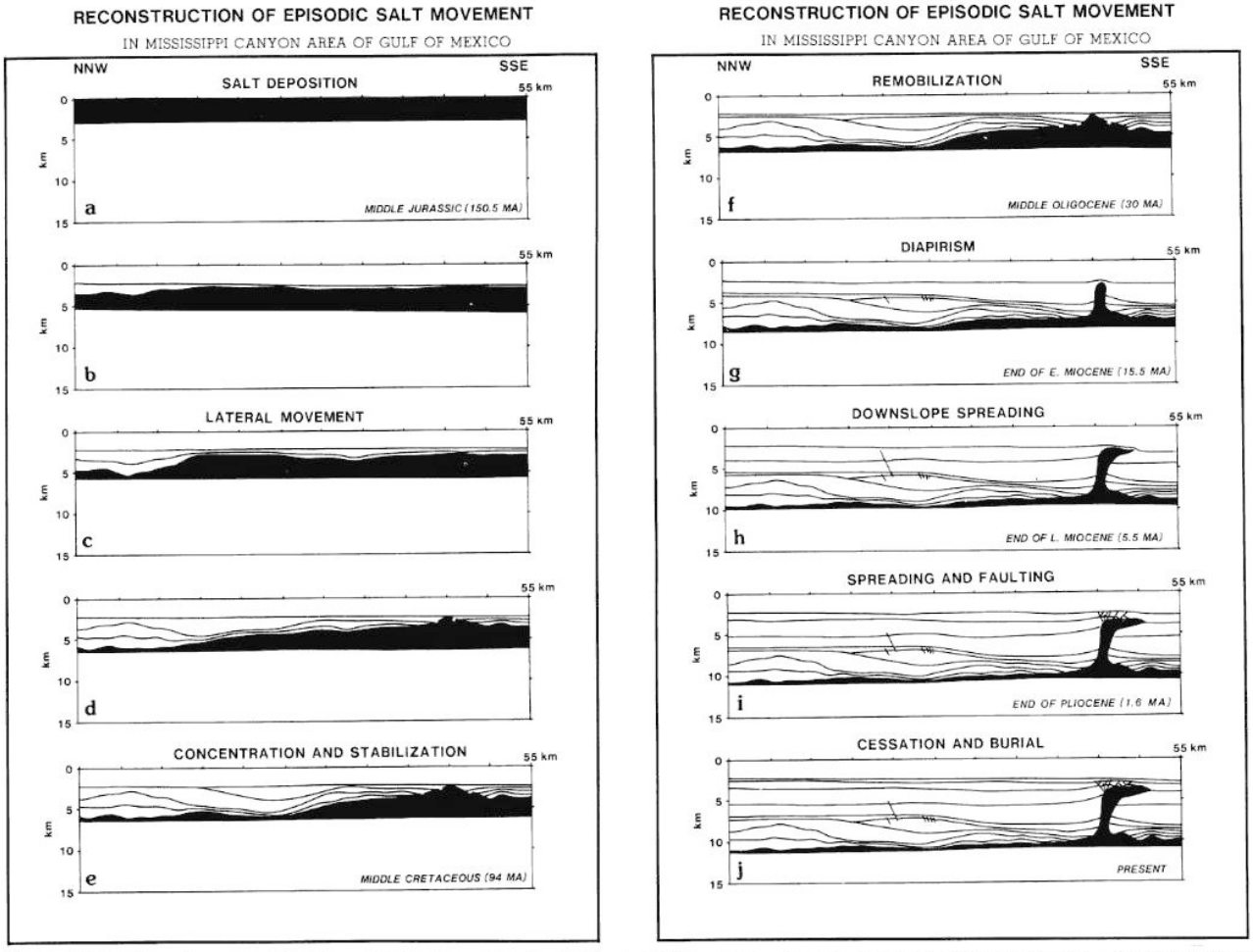

Figure 7 Hand-made reconstructions of depth section in *Foldout 3*. The section is assumed to be fixed in space. The areas of all sediments except salt are kept constant in the reconstructions. Decompaction is not taken into account. Note that the area of salt (black) cannot be balanced within the plane of the page. A significant amount of salt moved out of the plane of the section. Salt is assumed to occupy all space between the base of the autochthonous salt and the base of sediments overlying salt in the reconstructions. (a)–(e) show a period of salt concentration from Late Jurassic (TS) to end of Lower Cretaceous (TLC) by basinward salt movement due to upslope sediment load. Growth faults dipping both landward and seaward started to develop at (d). A minimum thickness of about 2.6 km is estimated for the original Louann Salt in (a). (e) and (f) show a long period of stabilization of salt structure due to starved sedimentation and later minimal remobilization of salt. (g) shows the time interval from Late Oligocene when the salt structure grew vertically due to the increase of sediment loads on top of the previously concentrated salt. (h) and (i) show a period of basinward spreading of salt from Middle Miocene to Early Pliocene. Faulting of the sediments over the feeder stock is shown in (i). (j) shows the present salt tongue which has virtually stopped spreading

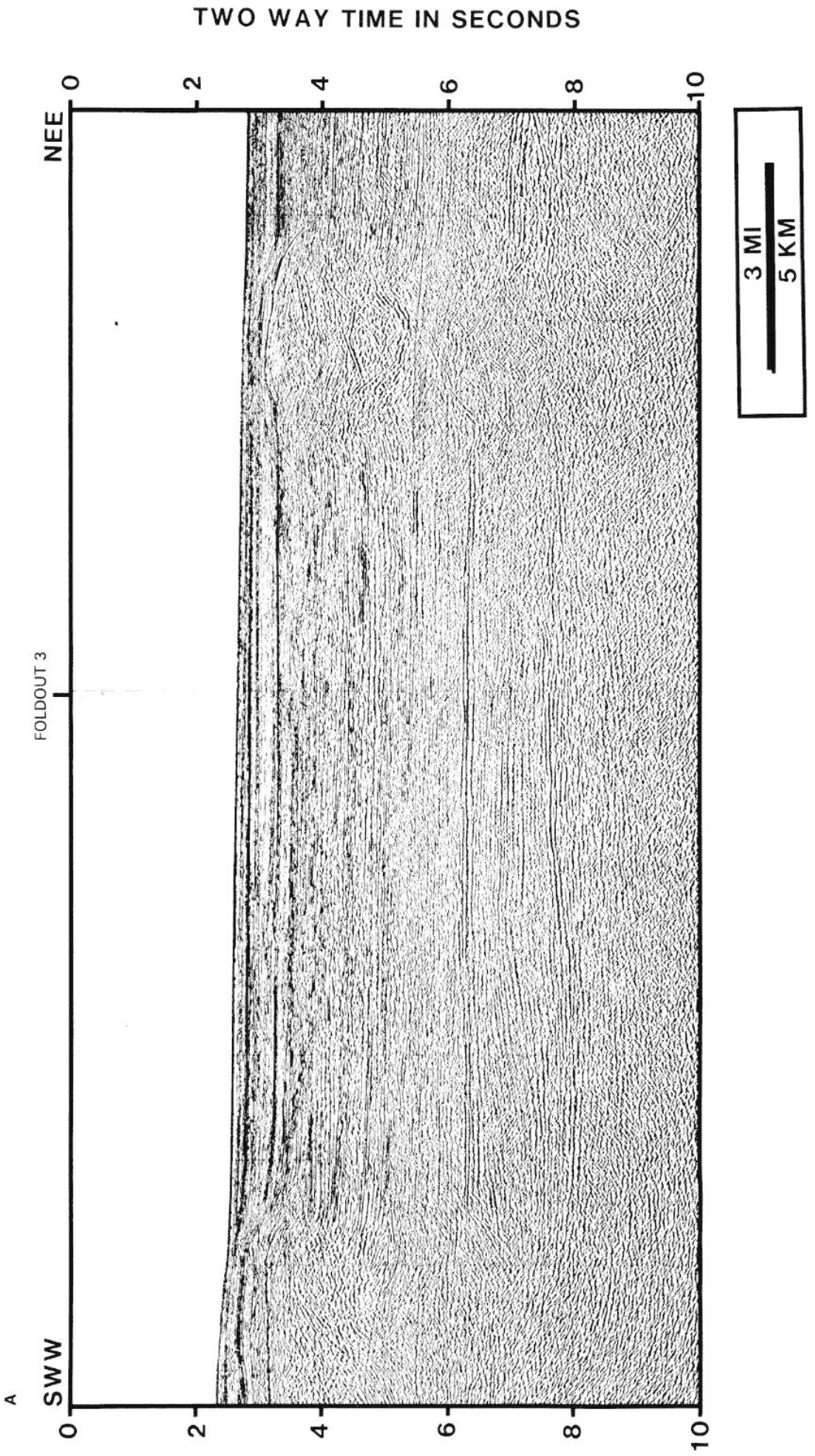

Figure 8 (A) Uninterpreted seismic profile perpendicular to *Foldout 3* (courtesy of GECO). For location see *Figure 11*. Part **(B)** is on the following page

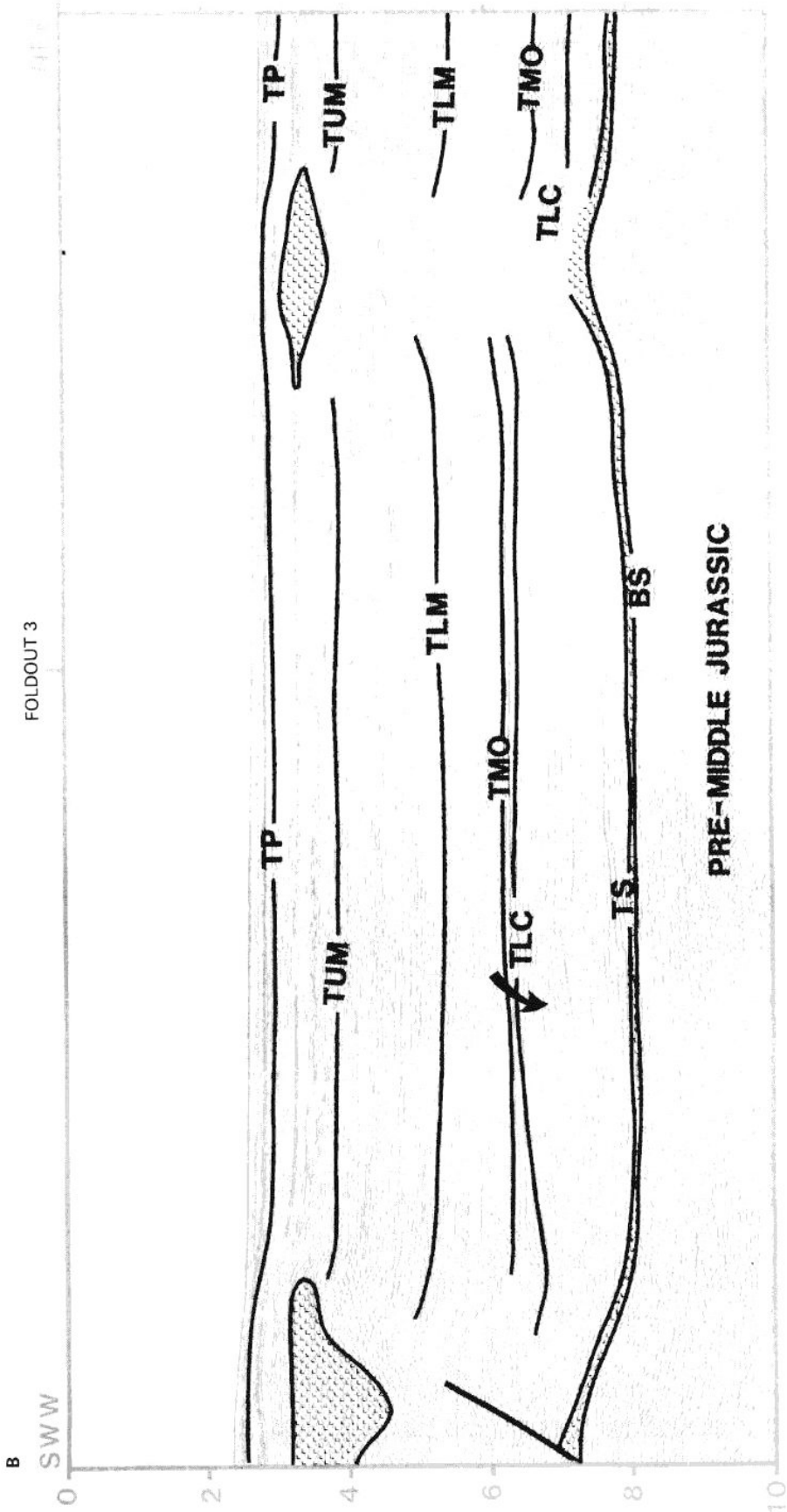

Figure 8 cont. **(B)** Interpreted seismic line in (A). The pseudo-clinoformal patterns between TS and TLC dipping SWW basinward show another component of basinward movement of salt which contributed to the out of plane movement of salt in *Figure 7* during the TS–TLC period

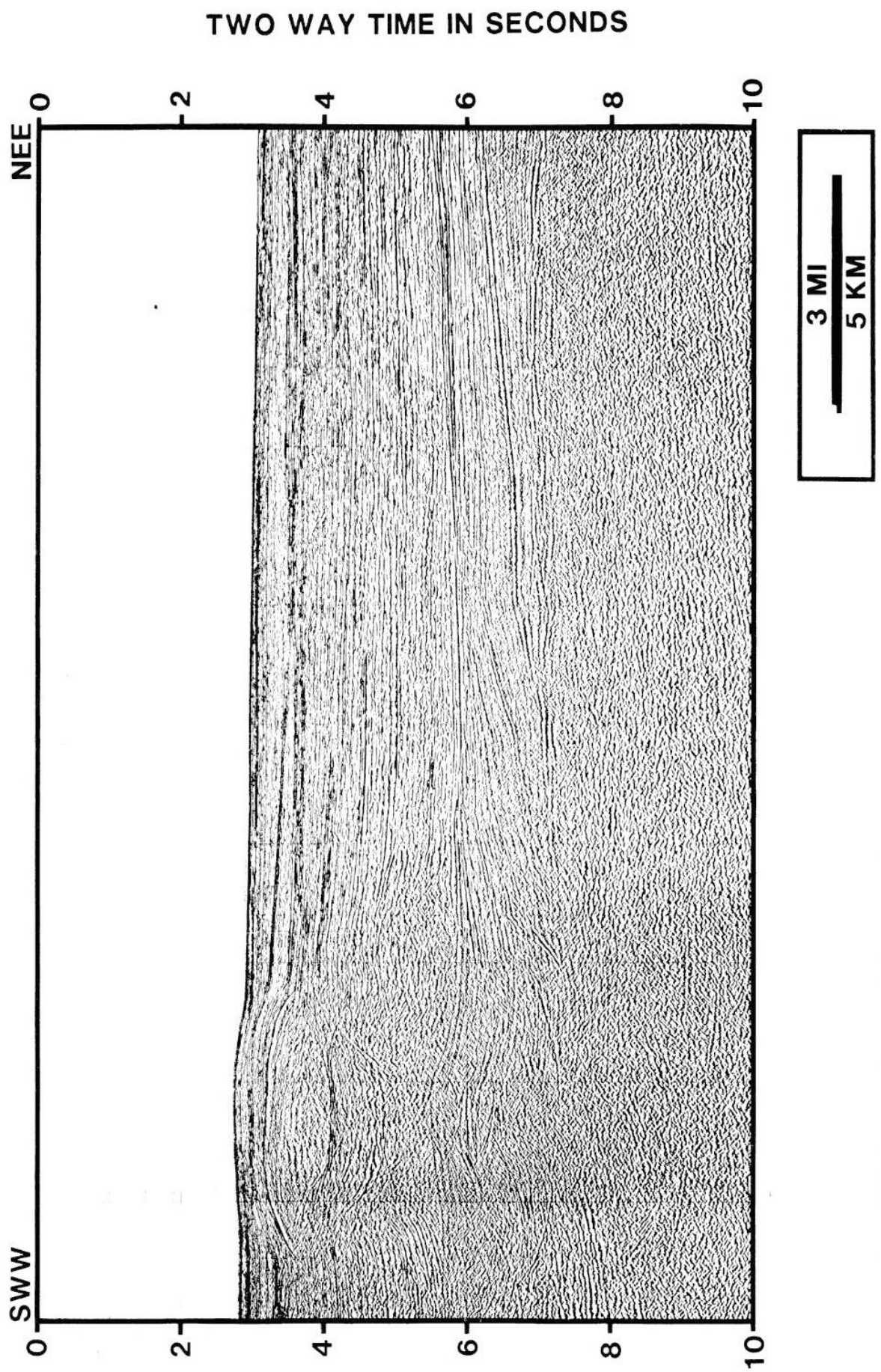

Figure 9 **(A)** Uninterpreted seismic profile landward of *Figure 8* (courtesy of GECO). For location see *Figure 11*. Part **(B)** is on the following page

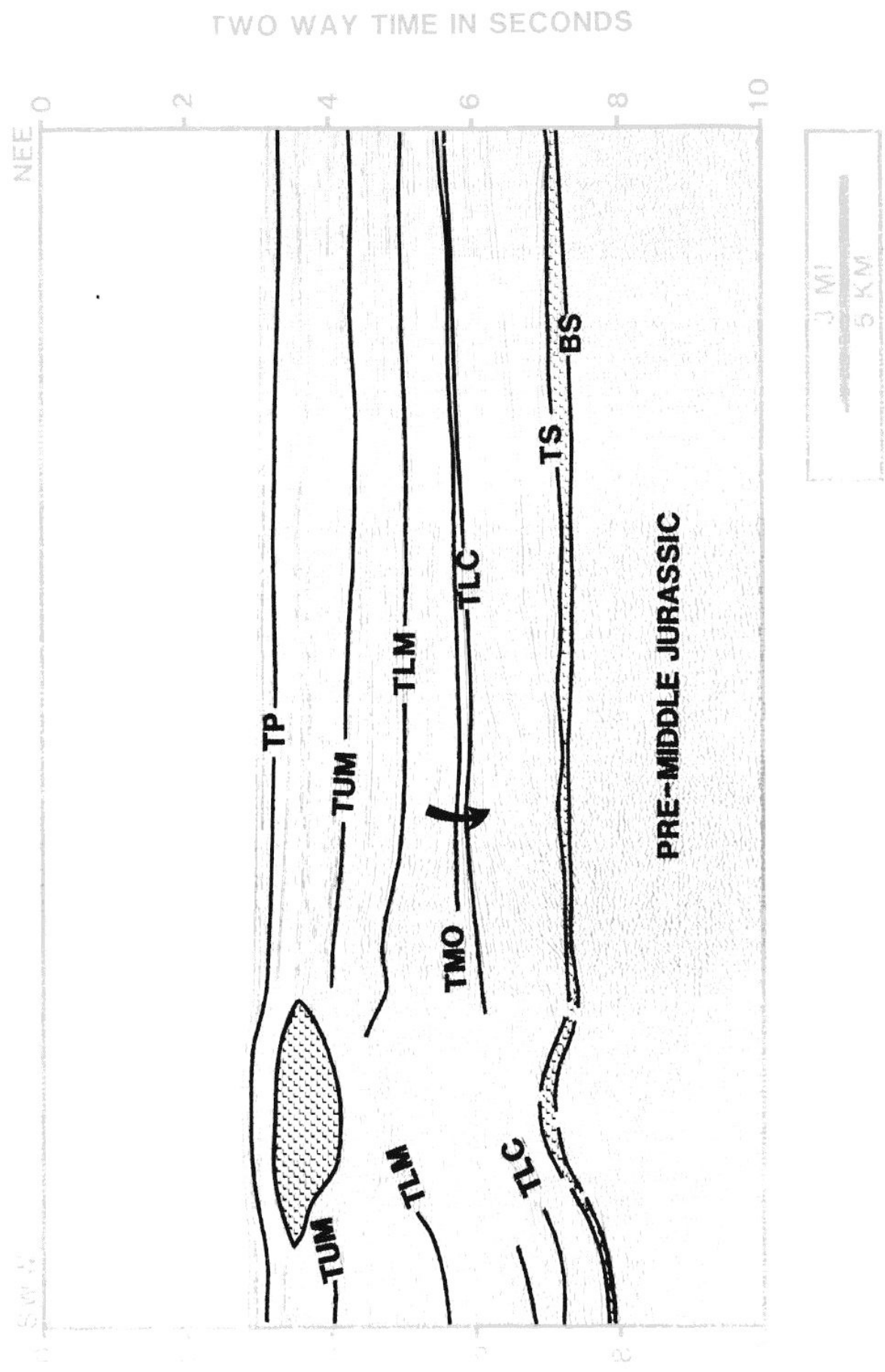

Figure 9 cont. **(B)** Interpreted seismic line in (A). The pseudo-clinoformal patterns dipping SW W away from land show the movement of salt away from land during TS–TLC period

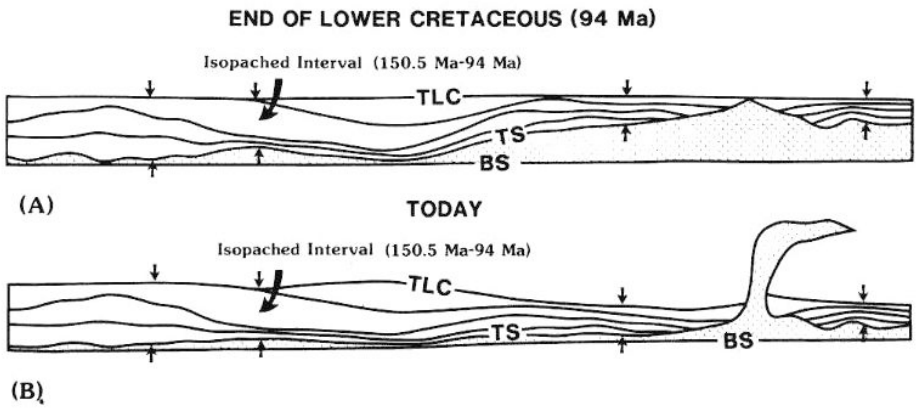

Figure 10 True scale present day cross-sections and reconstruction at the end of the Lower Cretaceous enlarged from the reconstructions of *Figure 7*. BS, Base of Werner Anhydrite and Louann Salt, 158.5 Ma sequence boundary; TS, top of Louann Salt, 150.5 Ma sequence boundary; TLC, top Lower Cretaceous, 94 Ma sequence boundary. By measuring the section between TS and TLC, a relative distribution of salt at the time of TLC can be estimated. Relatively thick salt at TLC is estimated from a thin interval of TS–TLC and *vice versa*. This estimate assumes a relatively flat bathymetry and base of autochthonous salt (BS) *(Figure 4)* and no regional extension at TLC time. Salt structures stabilized during the starved sedimentation following the Middle Cretaceous flooding events

shown on a seismic profile between TLC (94 Ma) and TS (150.5 Ma) in *Foldout 3*. At the first glance, it is not clear whether the stratal patterns are depositional or due to salt movement. In *Figure 6*, part of this clinoformal pattern is compared with a classical example of typical carbonate progradations of the Lower Cretaceous from the Vernon parish, Louisiana area (Tyrrell, Jr. and Scott, 1988). Note that the true dip of the pseudo-clinoforms in the example from the study area is twice that of those in the known shallow water carbonate system. Also the overlying sediments in the example from our study area show a syncline and expansion of thickness between TLC and TLM *(Foldout 3)* that are not seen in the known carbonate example *(Figure 6B)*. Regional sequence stratigraphic analysis suggests that the pseudo-clinoforms of *Foldout 3* are possibly composed of off-reef lowstand and distal highstand system tracts. Our understanding is that the pseudo-clinoformal patterns in *Foldout 3* indicate periods of salt movements due to sediment loading in a carbonate slope environment and to withdrawal of salt as illustrated by our approximate two-dimensional palinspastic reconstructions *(Figure 7)*. A similar interpretation was applied by Jackson and Cramez (1989) to another example of apparent down-lap or pseudo-clinoforms. Decompaction is not included in the reconstructions as very little is known about the lithology of the pseudo-clinoforms. Thus during these early periods of movement, salt was concentrated in the slope environment by down-dip movement towards the deep Gulf of Mexico under the load of sediments that prograded basinward since 150.5 Ma. The reconstructions of *Foldout 3* shown in *Figure 7a–e* demonstrate salt movements during the period 150.5–94 Ma. The reconstruction is conducted by preserving the areas of the sediments except salt, as salt can not be balanced in two-dimensions due to its out of plane movement. Salt is assumed to fill all the space between the base of autochthonous salt and the base of overlying sediments. Growth faults both dipping towards and away from land were developed on top of the salt as the salt concentrated in the down-slope direction *(Figure 7d* and *e)*. An original salt thickness of at least 2.5–3 km is estimated from the reconstruction. Out of plane movement of salt has to be considered to balance all sedimentary sections. Such out of plane movement of salt can be visualized on a profile *(Figure 8)* perpendicular to *Foldout 3*. *Figure 8* shows similar pseudo-clinoformal patterns dipping towards the deep Gulf. Another seismic profile *(Figure 9)* located up-slope from *Figure 8* also shows the pseudo-clinoformal patterns that are believed to be due to lateral basinward salt movement.

The mobility of salt makes it very difficult to estimate the original distribution and thickness of the salt. However, the extensive condensed sedimentation related to Middle Cretaceous flooding events allows an indirect estimation of the palaeo-distribution of salt at 94 Ma. When the basin was flooded during the Middle Cretaceous as documented by the Middle Cretaceous Flooding Surface (MCFS, see Wu *et al.* (1990)), the starved sedimentation allowed the salt structures to stabilize during an extended period (94–30 Ma). *Figure 7e* and *f* suggest that there is little growth, if any, of salt structures during 94–30 Ma because the sedimentation was starved in the study area. Thus it is assumed that a relatively undisturbed surface existed during the times of very slow rates of sedimentation. The thickness distribution of salt at 94 Ma is inferred from the thickness of the sediments above the non-diapiric autochthonous salt (150.5 Ma sequence boundary, TS in the interpretations) and below the 94 Ma sequence boundary (TLC in the interpretations). Salt itself cannot be used for this estimation as it has moved since 94 Ma. A relatively flat salt base (BS in our interpretations) is assumed *(Figure 10)* for all our reconstructions. The sediments between TS and TLC are assumed to be close to their original depositional position and have a constant area during the Neogene if compaction effects are ignored. Using these assumptions, a relative palaeo-salt distribution at 94 Ma is indicated by an isopach map of the TS (150.5 Ma)–TLC (94 Ma) sediment interval *(Figure 11)*. Relatively thick palaeo-salt concentrations at 94 Ma are suggested by relatively thin sediments on top of the salt. It needs to be emphasized that the inferred thickness of the salt is relative and indicates only the minimum thickness. The map shows that by 94 Ma, salt was distributed in the form of large salt pillows, domes and irregular salt massifs. In conclusion, the Early

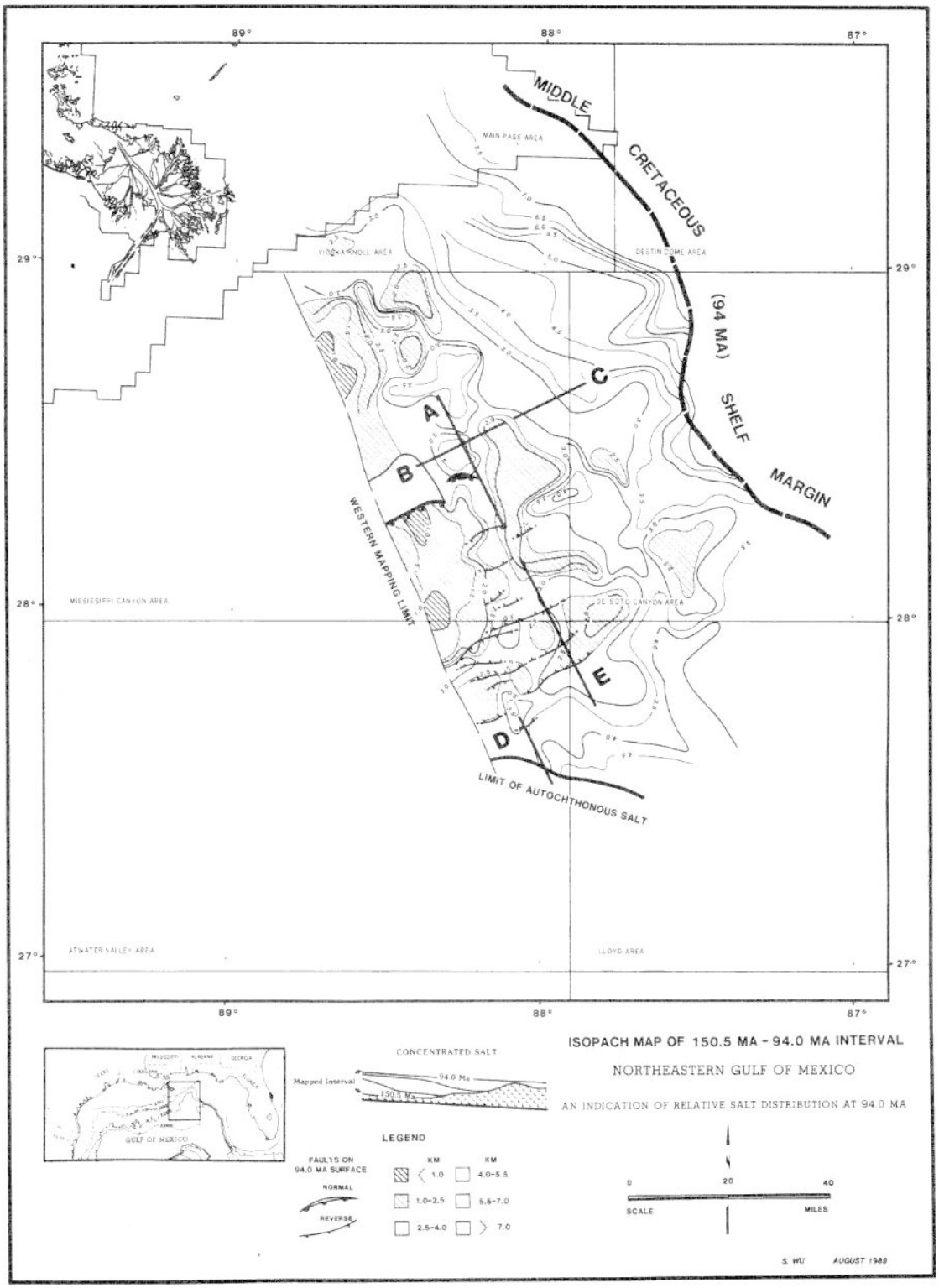

Figure 11 Isopach map of TS–TLC interval and the locations of seismic examples. Line A, *Foldout 3;* Line B, *Figure 8;* Line C, *Figure 9;* Line D, *Figure 22;* Line E, *Foldout 6.* As explained in *Figure 10,* relatively thick salt is indicated by the thin isopached interval. Shaded areas indicate primary pre-Mid Cretaceous salt pillows. These concentrated salt masses later contributed to the formation of allochthonous salt during the Neogene

Cretaceous primary concentration of salt in the slope areas formed vast structural feeder mounds and stocks that later provided a large amount of salt to the allochthonous salt tongues and sheets evolved in the slope environment during the Neogene.

Late Cretaceous and Palaeogene remobilization of salt

During the Late Cretaceous and Palaeogene, sediments began prograding into the slope area *(Foldouts 2–4* of Wu *et al.* (1990)). Increased sediment loads remobilized the salt. However, because our area was far to the east of the Late Cretaceous and Palaeogene depocentres of the north-western Gulf of Mexico, the rate of sedimentation still remained very low. In the seismic example in *Foldout 3*, on average there was less than 1 km of sediment deposited in the slope area during a period of 64 Ma (94–30 Ma). Thus the sediment accumulation rate was about 15 m Ma^{-1}. The reconstructions of *Figure 7e* and *f* show only a limited growth of salt structures. By Mid-Oligocene, there was a first major low stand sediment influx *(Foldouts 2–4* of Wu *et al.* (1990))into the slope area. The lowstand influx induced a significant amount of salt growth.

Neogene–Quaternary development of allochthonous salt

The rates of sediment accumulation have increased rapidly since the Early Miocene as a consequence of progradation of the shelf margins and the shifting of depocentres into our study area. Thus about 2 km of sediments accumulated in the slope area *(Foldout 3* and *Figure 7g)* during a period of about 15 Ma (30–15.5 Ma) at a rate of 130 m Ma^{-1}, i.e. about one order of magnitude greater than the rate of 15 m Ma^{-1} during 94–30 Ma. This induced a period of diapirism and rapid relative upward growth of salt structures as illustrated in the palinspastic reconstructions shown in *Figure 7*. A high pressure gradient due to density inversion forced the salt to move relatively upwards.

The rapid relative upward growth of salt structures which began during the Late Oligocene and/or Early

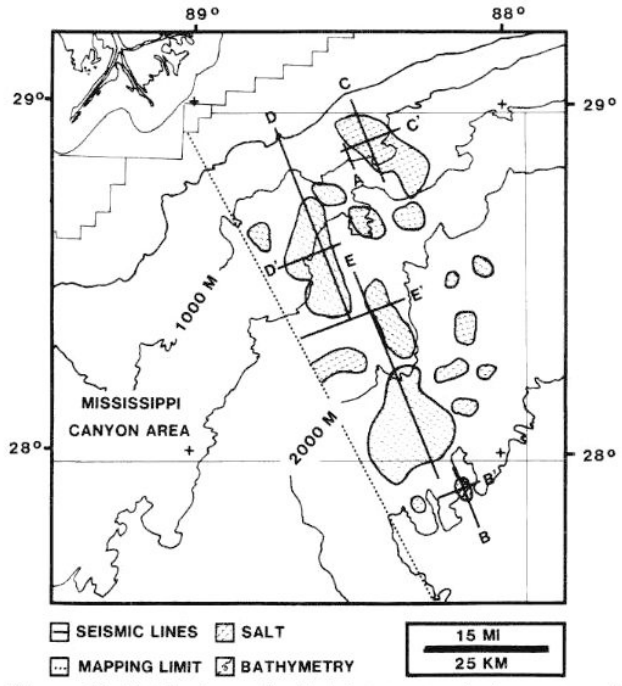

Figure 12 Distribution of allochthonous salt tongues and sheets and the location of seismic profiles showing the evolutionary stages of allochthonous salt in the northeastern Mississippi Canyon Area. Seismic lines are Line A, *Figure 13;* Line B, *Figure 14;* Line B', *Figure 15;* Line C, *Figure 16;* Line C', *Figure 18;* Line D, *Foldout 4;* Line D', *Figure 19;* Line E, *Foldout 5* and Line E', *Figure 20*

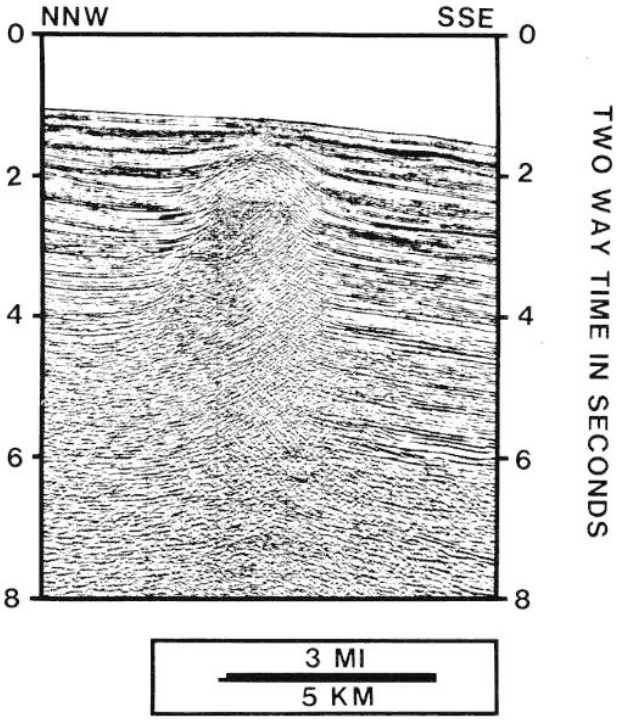

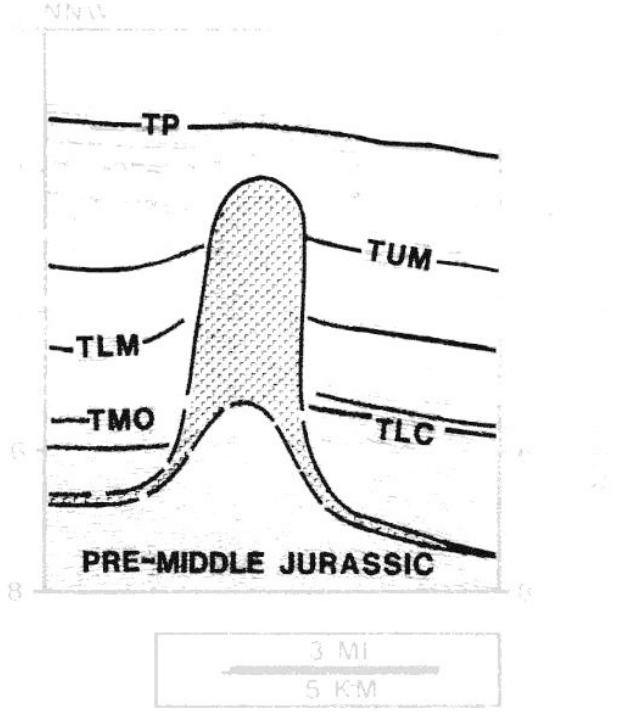

Figure 13 (A) Uninterpreted seismic example of a diapiric salt dome (courtesy of GECO). For location see *Figure 12.* **(B)** Interpreted example of (A). The salt structure in this example is interpreted as one of structures of the Autochthonous Salt Stage in the evolution of allochthonous salt

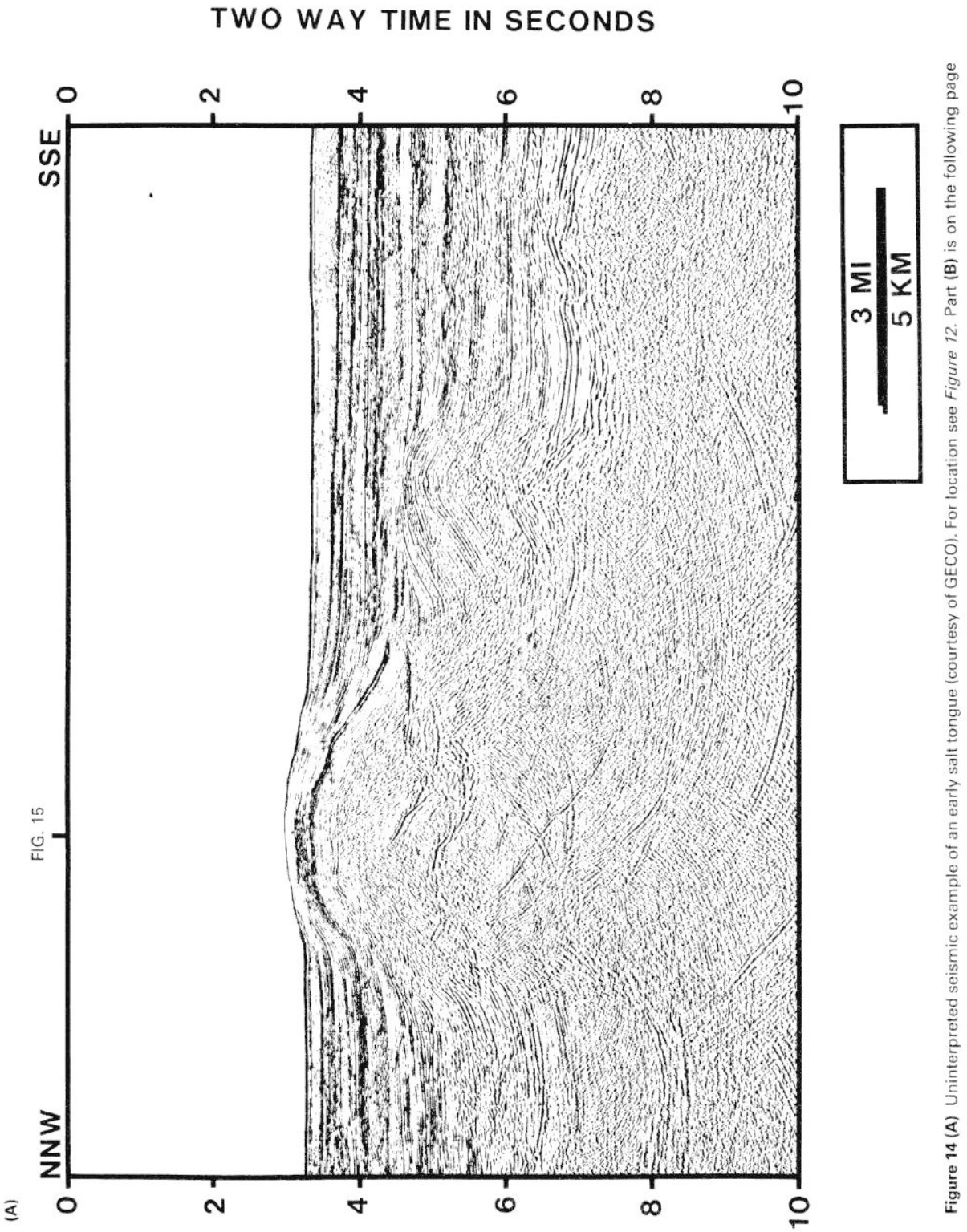

Figure 14 (A) Uninterpreted seismic example of an early salt tongue (courtesy of GECO). For location see *Figure 12*. Part **(B)** is on the following page

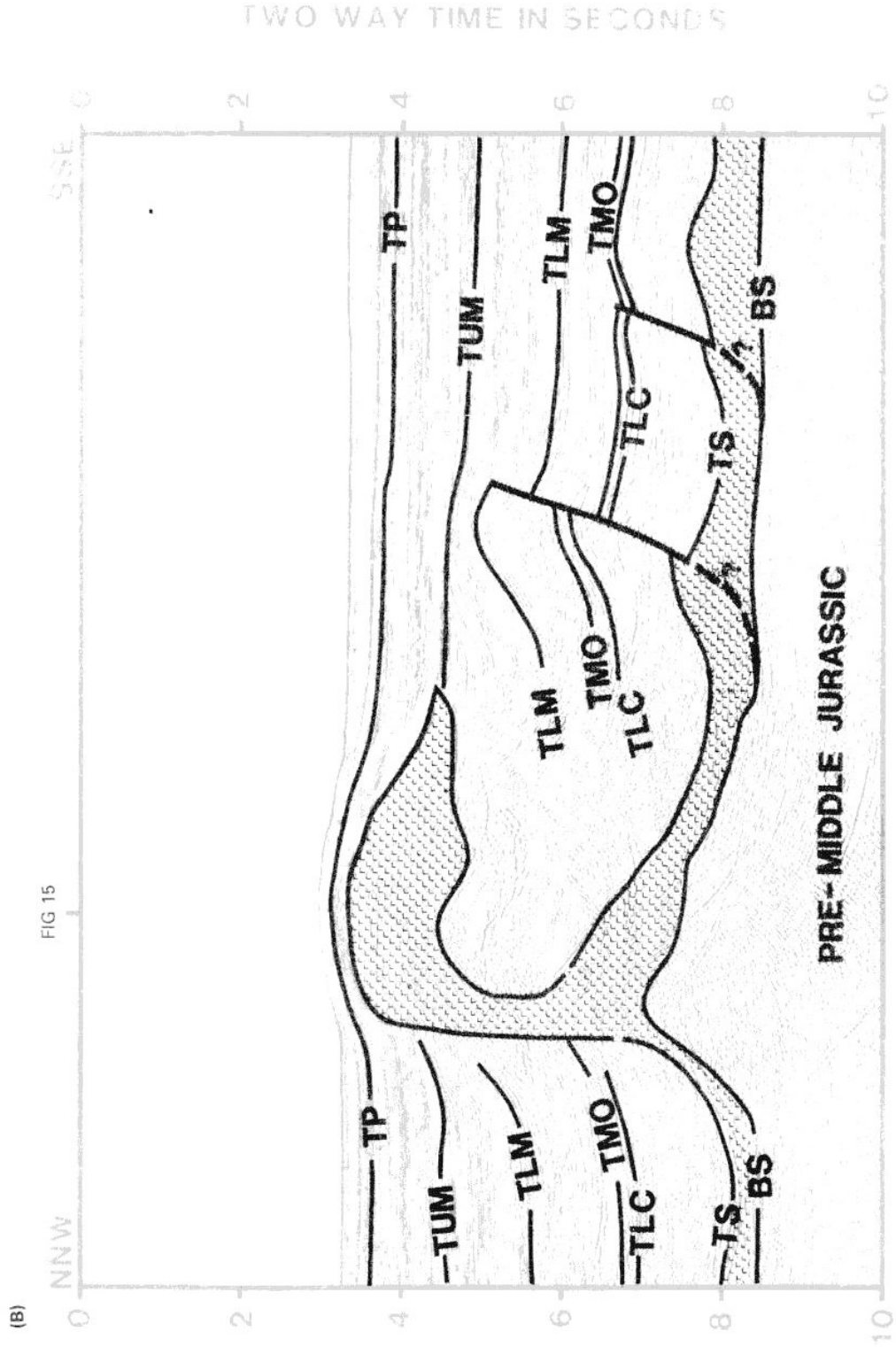

Figure 14 (B) Interpreted example of (A). The salt structure in this example is interpreted as one of the early salt structures of Allochthonous Salt Stage of the evolution of allochthonous salt. Note that salt tongue spreads in the down-slope direction within Upper Miocene and Pliocene sediments. A bathymetric high is observed over the salt tongue

Miocene continued into the Upper Miocene. Since the Middle Miocene, salt flowed laterally within the Neogene sediments as shown in *Foldout 3* and the reconstructions in *Figure 7*. A sedimentation rate of 180 m Ma^{-1} is estimated for the period 15.5–1.6 Ma. Lateral spreading of salt continued into the Plio–Pleistocene. A system of fault patterns developed in the sediments overlying the feeder stock as the salt supply decreased. In the specific example of *Foldout 3*, lateral spreading of the salt tongue ceased by the end of the Pliocene (1.6 Ma).

In summary, *Foldout 3* and the palinspastic reconstructions in *Figure 7* document the timing of salt movement typical for the slope study area since the deposition of the Jurassic Louann Salt (150.5 Ma or TS). A period of basinward salt movement during 150.5–94 Ma towards the deep basin ended with a first concentration of salt in feeder mounds within the present-day slope environment *(Figure 7a–f)*. An extended period (94–30 Ma) of starved sedimentation associated with 93.5 and 91.5 Ma flooding events allowed the salt structures to stabilize *(Figure 7e)*. A rapid influx of sediment since the Late Oligocene and Early Miocene (30–15.5 Ma) caused a period of diapirism and relative upward growth of salt structures *(Figure 7g)*. Spreading of allochthonous salt within younger sediments then occurred from the Middle Miocene (15.5 Ma) to the Plio–Pleistocene *(Figure 7h–j)*.

Evolutionary stages of allochthonous salt

In this section the autochthonous salt, the allochthonous salt and detached allochthonous salt are interpreted as the evolutionary stages of a typical allochthonous salt sheet. Seismic examples from our study area illustrate each of the evolutionary stages associated with an allochthonous salt sheet. We view the structures in each of the following examples as frozen stages of the evolution of allochthonous salt sheets. A map in *Figure 12* shows the distribution of allochthonous salt tongues and sheets and the location of the seismic examples in our slope study area.

Autochthonous salt stages represent the earliest salt deformation in the evolution of an allochthonous salt sheet. During the autochthonous salt stages, salt rollers, swells, anticlines and domes *(Foldout 2;* Jackson and Talbot, 1986) are typically developed. Autochthonous salt structures were dominant in the study area during the period 150.5–30 Ma. As sediment loads increased, salt swells, anticlines and domes developed into diapiric salt walls and domes. An example of a diapiric salt dome from the study area is shown in *Figure 13*. Growth of autochthonous salt structures dominated during the period 30–15.5 Ma, corresponding to the increased influx of sediments into the study area *(Figure 7g)*. The growth of the dome in *Figure 13* ended in the Pliocene when the salt supply to the dome was depleted. As long as there was sufficient salt supply, salt continued to develop into the next stages.

Allochthonous salt stages begin when salt is emplaced within stratigraphically younger sediments. The allochthonous salt is illustrated in *Figures 14–17*. *Figures 14* and *15* show an early stage salt tongue which spreads in the down-slope direction. The top of the salt is overlain by approximately 300 m of sediments. A bathymetric high over the tongue is observed. An allochthonous salt tongue developed as the salt moved up through the feeder stock and reached the level of dynamic equilibrium. The spreading of salt also requires that there is enough salt available to form the tongue. The sediments in the slope environment, where most of the allochthonous salt tongues are formed, are weak enough so that salt can emplace within the sediments. The bathymetric high over the salt tongue indicates that the feeder stock is deeply rooted and still actively supplying salt to the tongue. The elevated salt tongue is supported by the pressure gradient in the deeply rooted feeder stock. When developed in a slope environment, a salt tongue preferentially spreads in the down-slope direction due to the gravity component parallel to the slope. The very presence of a slope enhances the spreading of salt and the formation of asymmetrical salt tongues *(Figures 14–16)*. The slope gradient may be further exaggerated by the subsidence of the sediments beneath the spreading tongue as salt is withdrawn from the original salt bed *(Figure 16C)*. The spreading of salt is further accelerated by the softening effect of water-wetted salt (the Joffée effect, Odé, 1968; Talbot and Rogers, 1980; Talbot and Jarvis, 1984; Jackson and Talbot, 1986; Talbot and Jackson, 1987a). The sediments overlying the salt tongue prevent the salt from being dissolved directly in sea water. However, the connate water in the sediments softens the salt. A spreading salt tongue within the sediments must overcome friction at the base and top of the tongue in addition to the strength of sediments in front of the tongue.

As salt spreads through time, newly deposited sediments will interact with the spreading salt tongue. *Figure 16* shows a salt tongue which has been further extended in the down-slope direction. The sediments overlying the salt tongue have been rotated in a counter-clockwise direction on top of the spreading salt. Sediments on top of the tongue have been dragged along with the salt tongue in the down-slope direction. The sediment loads on top of the salt further help the salt tongue to spread. The top of the salt tongue in *Figure 16* changes laterally from dipping seaward to landward. At the deepest part on top of the tongue, mechanical conditions of the salt tongue as a whole change from predominantly down-slope spreading to down-slope overthrusting. At the local minimum on top of the salt tongue, the overlying sediments are about 1400 m thick *(Figure 16C)*. The sediments are dense enough at this depth to generate a density inversion between the salt tongue and the overlying sediments (Jackson and Talbot, 1986). As the salt tongue spreads, it adapts to changing mechanical conditions to maintain a dynamic equilibrium. Thus the salt tongue climbs up the sedimentary section to balance the increased burial depth by overlying sediments. The salt tongue overthrusts and truncates flat-lying sediments deposited in front of and underneath it. The steplike base of the tongue *(Figures 16C* and *17)* indicates the episodic overthrusting of the tongue due to loading. A bathymetric high is produced over the thrusted part of the salt tongue whereas a bathymetric step forms at the frontal end of the tongue. *Figure 18* shows a seismic line perpendicular to *Figure 16* across the same tongue. Salt also spreads sideways as shown on this strike section. However, the spreading is much less than that seen in the structural dip section.

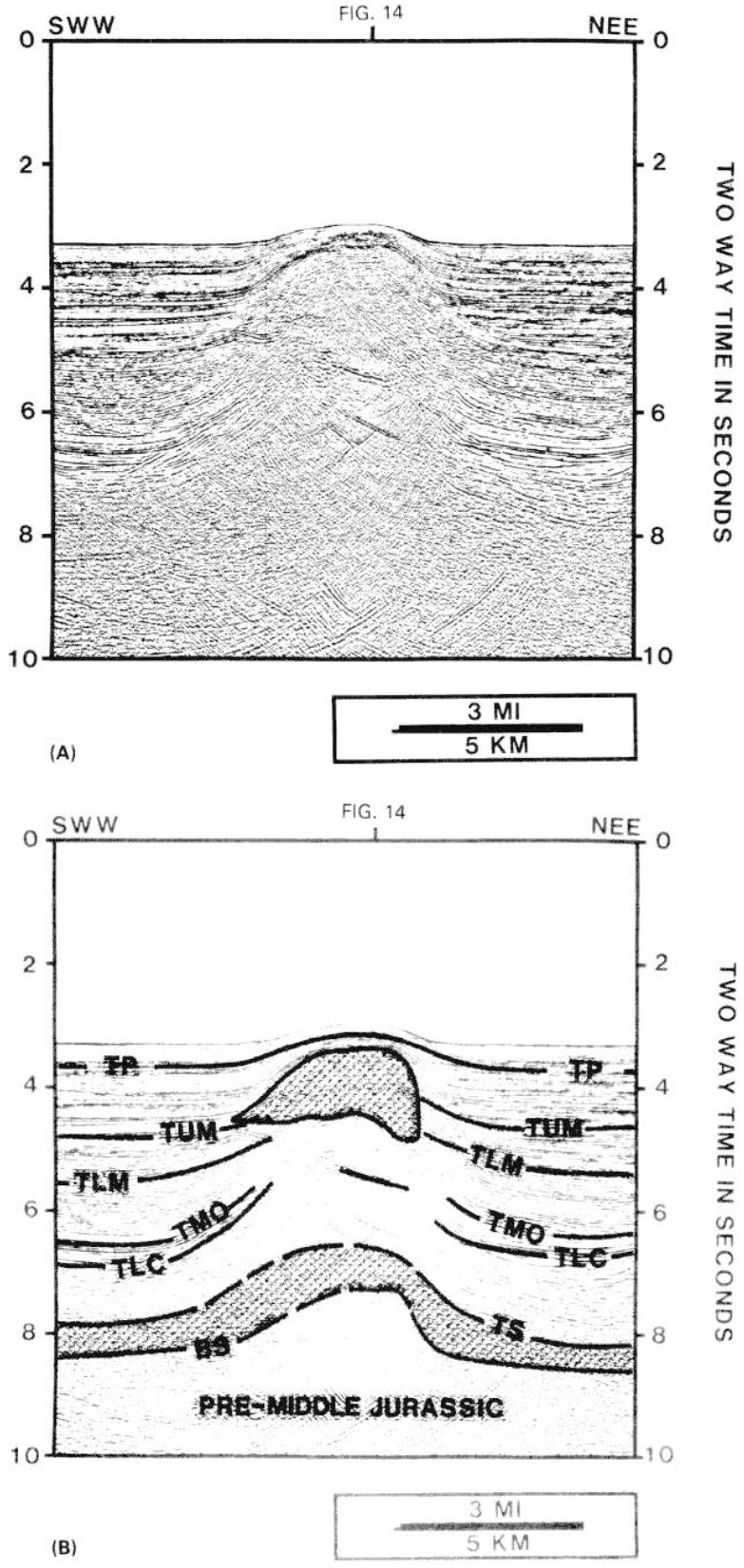

Figure 15 (A) Uninterpreted seismic example of early salt tongue perpendicular to *Figure 14 (courtesy of GECO).* For location see *Figure 12.* **(B)** Interpreted example of (A). Note that salt tongue spreads in the down-slope direction to the west. A bathymetric high is observed over the salt tongue

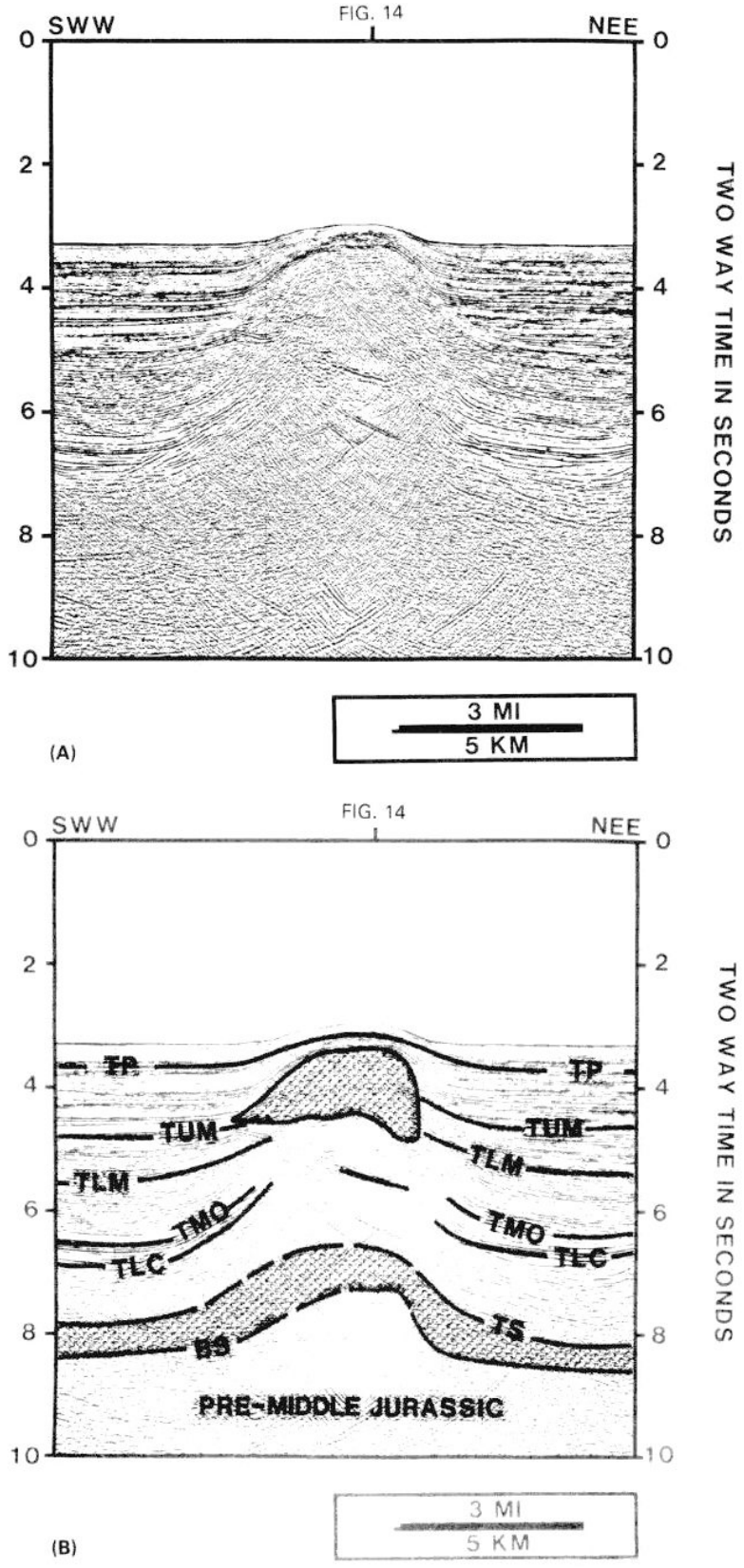

Figure 15 (A) Uninterpreted seismic example of early salt tongue perpendicular to *Figure 14 (courtesy of GECO).* For location see *Figure 12.* **(B)** Interpreted example of (A). Note that salt tongue spreads in the down-slope direction to the west. A bathymetric high is observed over the salt tongue

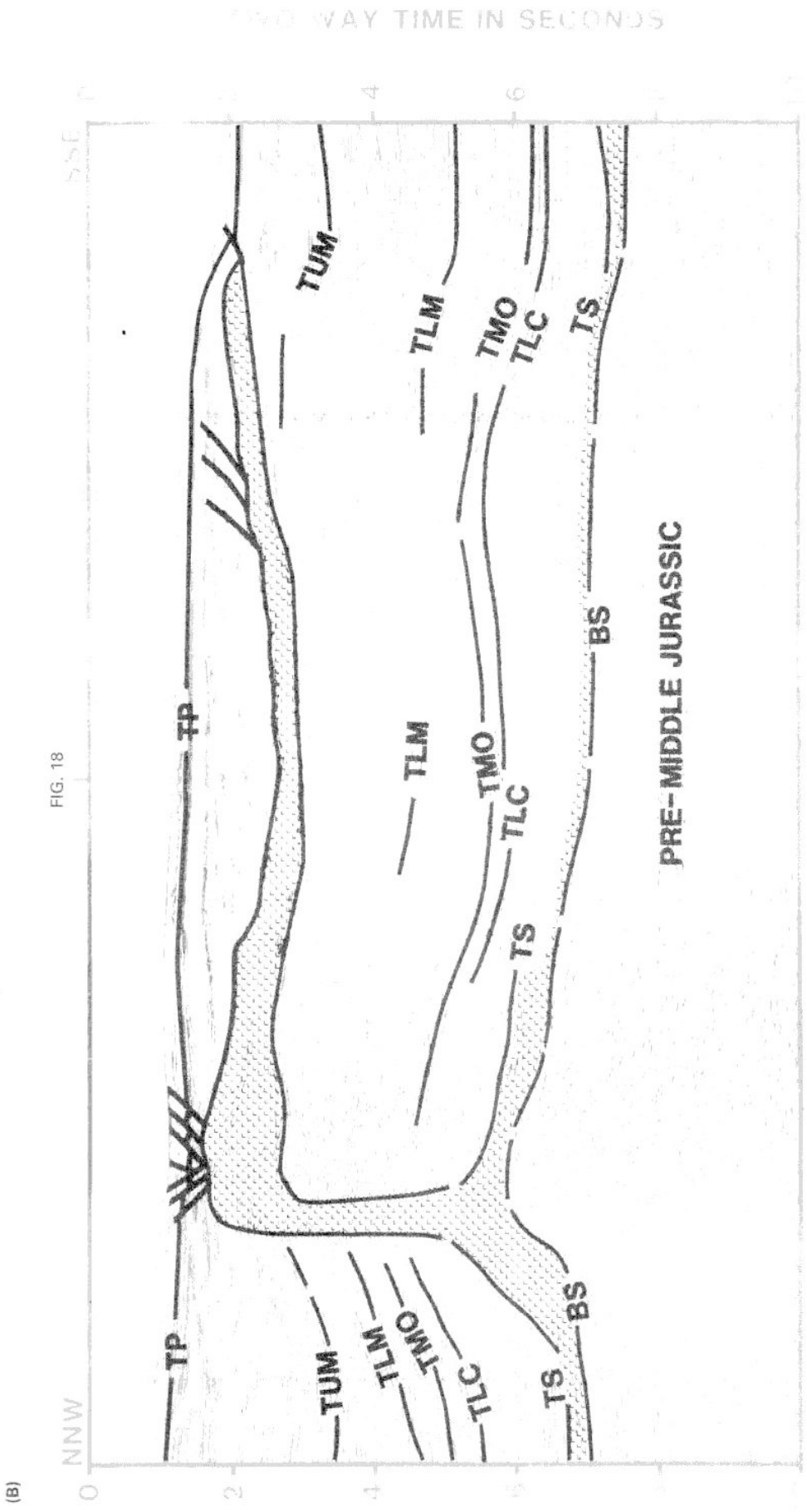

Figure 16 cont. **(B)** Interpreted seismic line in (A). This example is interpreted as one of the structures of Allochthonous Salt Stage of evolution of allochthonous salt

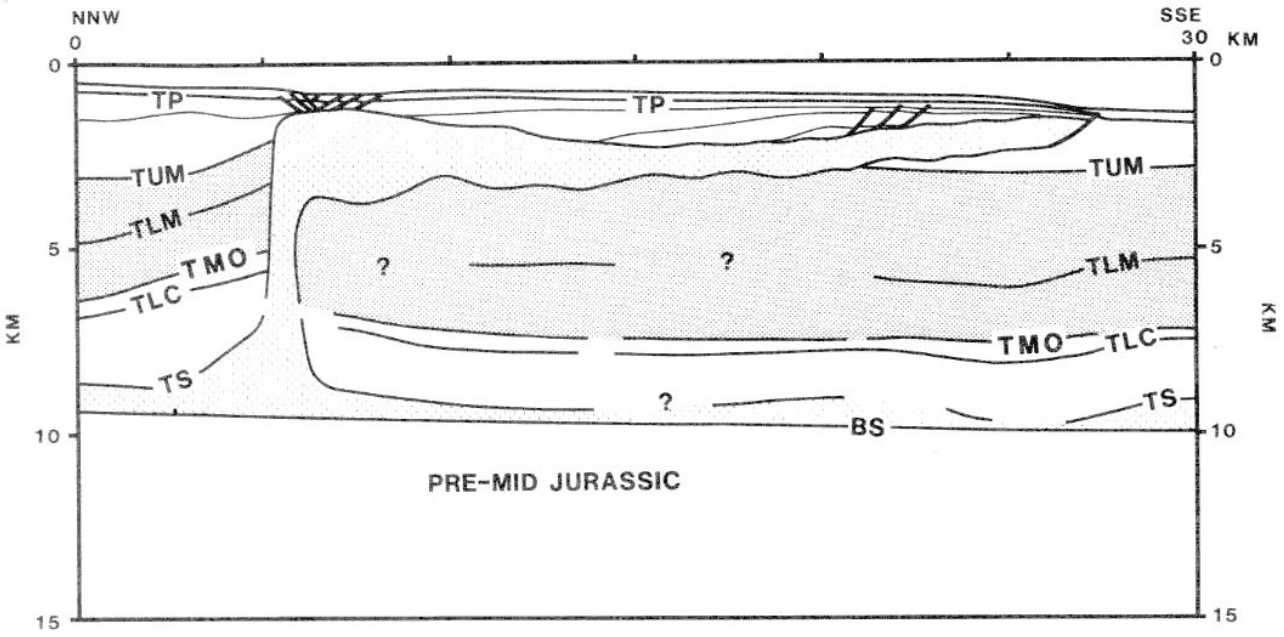

Figure 16 (C) Depth-covered section of (B). Interval velocities for depth conversion are in *Table 1.* Note that salt tongue spreads predominantly in the down-slope direction and the sediments on top of the tongue rotate mainly counter-clockwise as the tongue spreads. A bathymetric low and a set of faults are observed over the feeder stock due to decreasing pressure gradient in the feeder stock in the late stage of a salt tongue. Note the dip of top of salt tongue changes from basinward dipping (SSE) to landward dipping (NNW), indicating that the tongue as a whole changes from spreading down-slope to overthrusting down-slope. A critical point is defined at the point of the top-salt dip change. The step-like base of the tongue indicates episodic thrusting due to sediment loadings. A bathymetric high is observed over the thrusting part of the salt tongue. A set of landward dipping faults developed over the leading part of the tongue

The salt tongue in this example took about 5 Ma to spread to its present length of 22 km in the down-slope direction *(Figure 16C).*

The example of *Figure 16* also documents a system of faults associated with the down-slope spreading salt. A set of landward dipping faults developed over the basinward leading part of the salt tongue. This set of faults is due to the withdrawal of salt from the central part to the thrusted front of the tongue. Another system of faults develops in the sediments above the feeder stock and the thickest part of the salt tongue. Compared with the bathymetric high of the previous salt tongue example *(Figures 14* and *15),* a bathymetric low over the feeder stock in *Figure 16* now starts to develop. The faults and the bathymetric low suggest that the pressure gradient in the feeder stock decreased due to decreasing salt supply in the original salt bed. The pressures in the feeder stock no longer support the elevated salt mass above the feeder stock. Because the salt is spreading in the down-slope direction and sediments are coming from the land, down to the basin growth faults begin to develop predominantly. The interaction between spreading salt tongue and sediment load is summarized in *Figure 17.* As the salt over the feeder stock continues to collapse and as sediments continue to load in the bathymetric low above the feeder stock, the thick salt over the feeder stock is squeezed out into the frontal part of the salt tongue. The withdrawal of thick salt at the feeder stock accommodates the expanding overlying sediments. The extensive spreading of salt and the development of growth fault systems behind the salt tongue lead the allochthonous salt tongue into the detached allochthonous salt stages.

Detached allochthonous salt stages are the last stages in one cycle of the development of allochthonous salt.

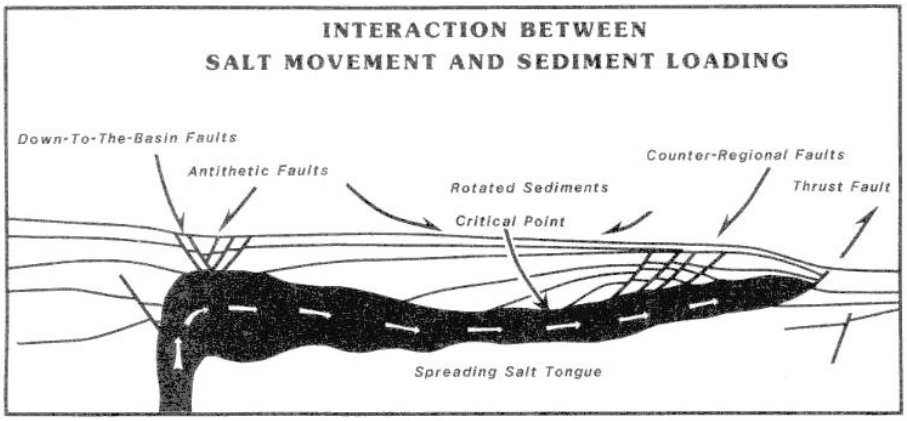

Figure 17 Schematic summary of the major features seen in *Figure 16*

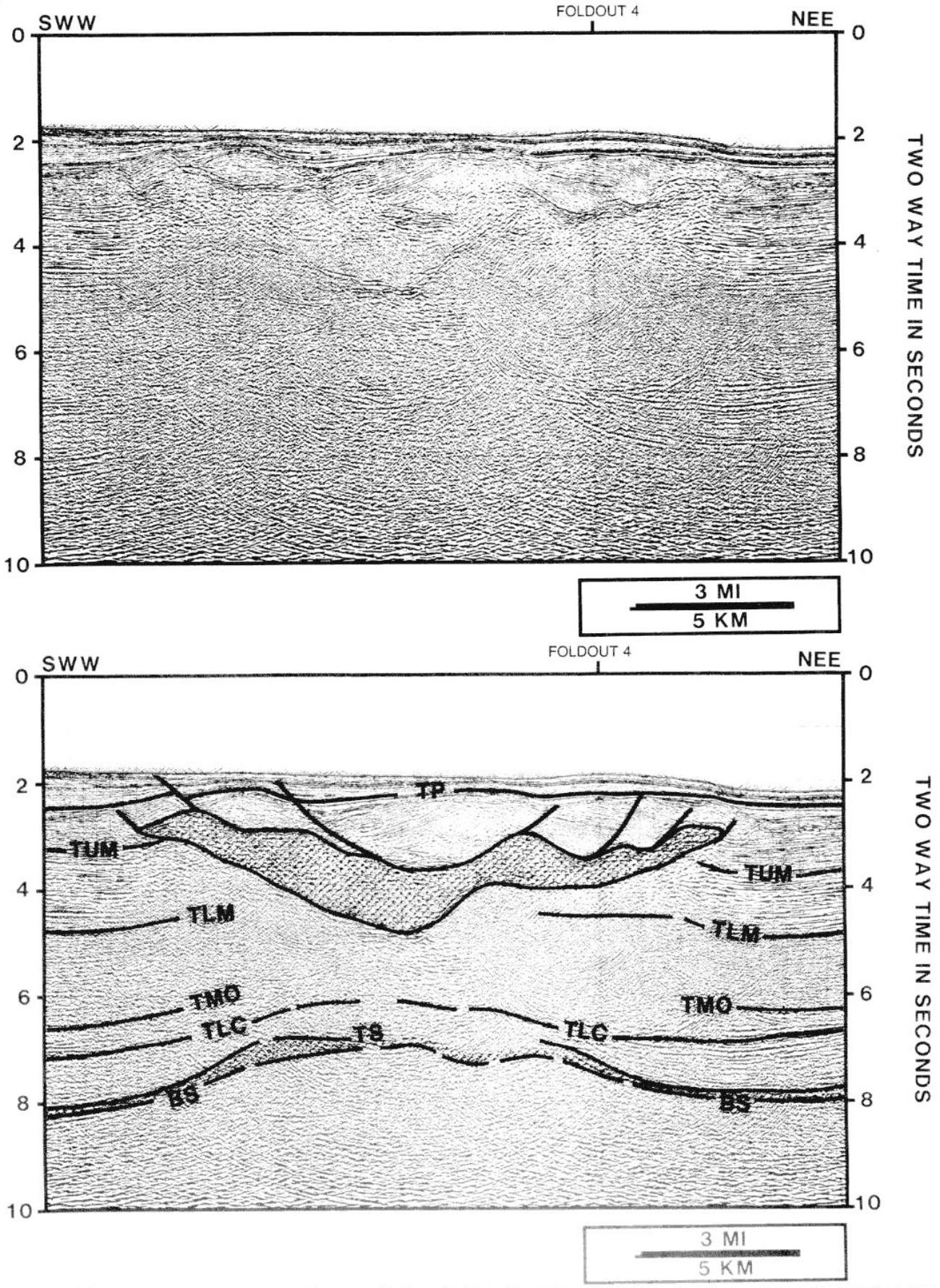

Figure 19 (A) Uninterpreted seismic example perpendicular to *Foldout 4* (courtesy of GECO). For location see *Figure 12*. **(B)** Interpreted example of (A). Note that the salt sheet spreads and thrusts sideways. Normal faults dipping down-slope are observed over the salt sheet on the left. A bathymetric step and normal faults dipping up-slope are observed over the sheet on the right. Faults developed over the tongue and soled out at the top of the salt sheet

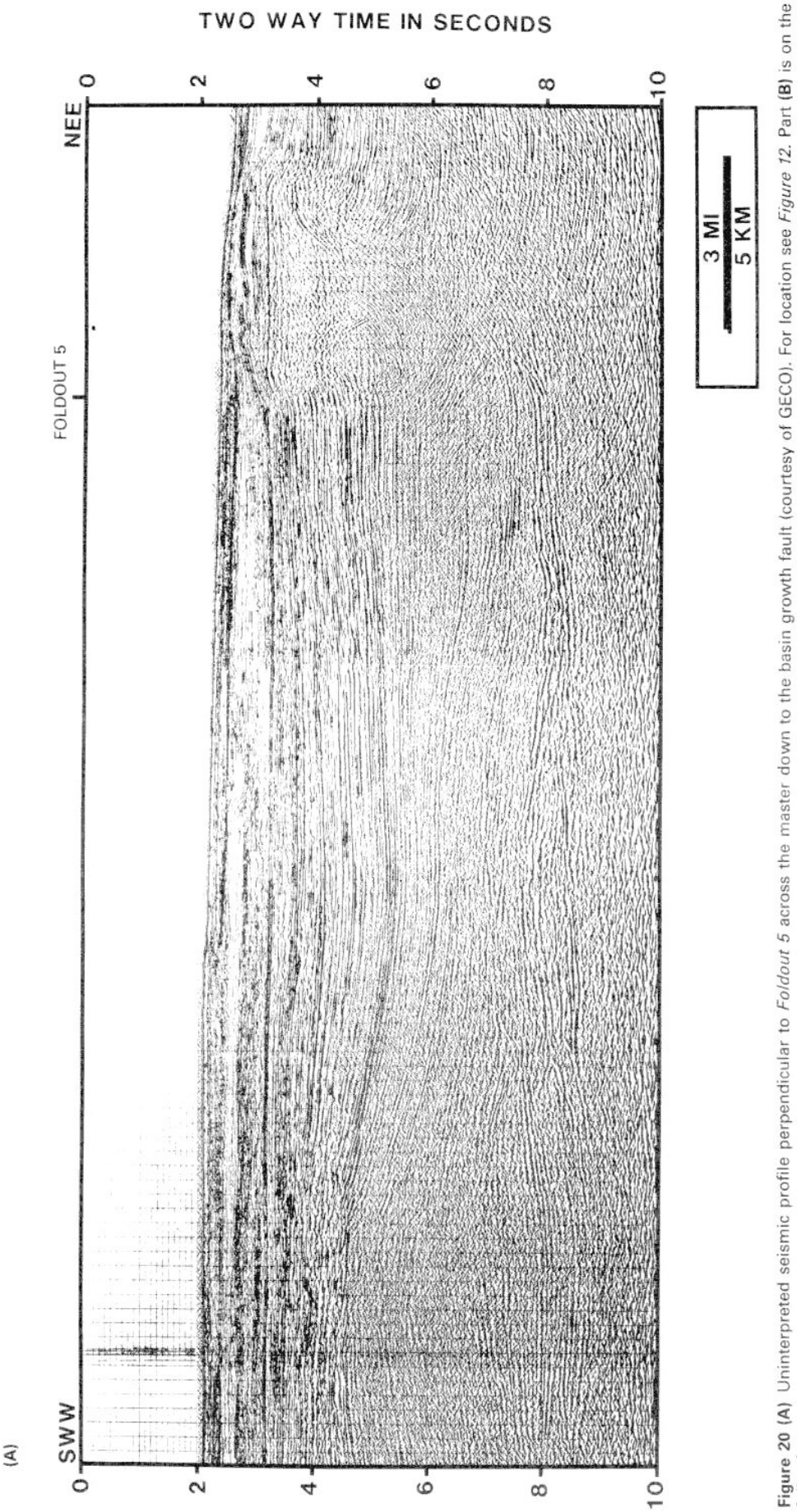

Figure 20 (A) Uninterpreted seismic profile perpendicular to *Foldout 5* across the master down to the basin growth fault (courtesy of GECO). For location see *Figure 12*. Part **(B)** is on the following page

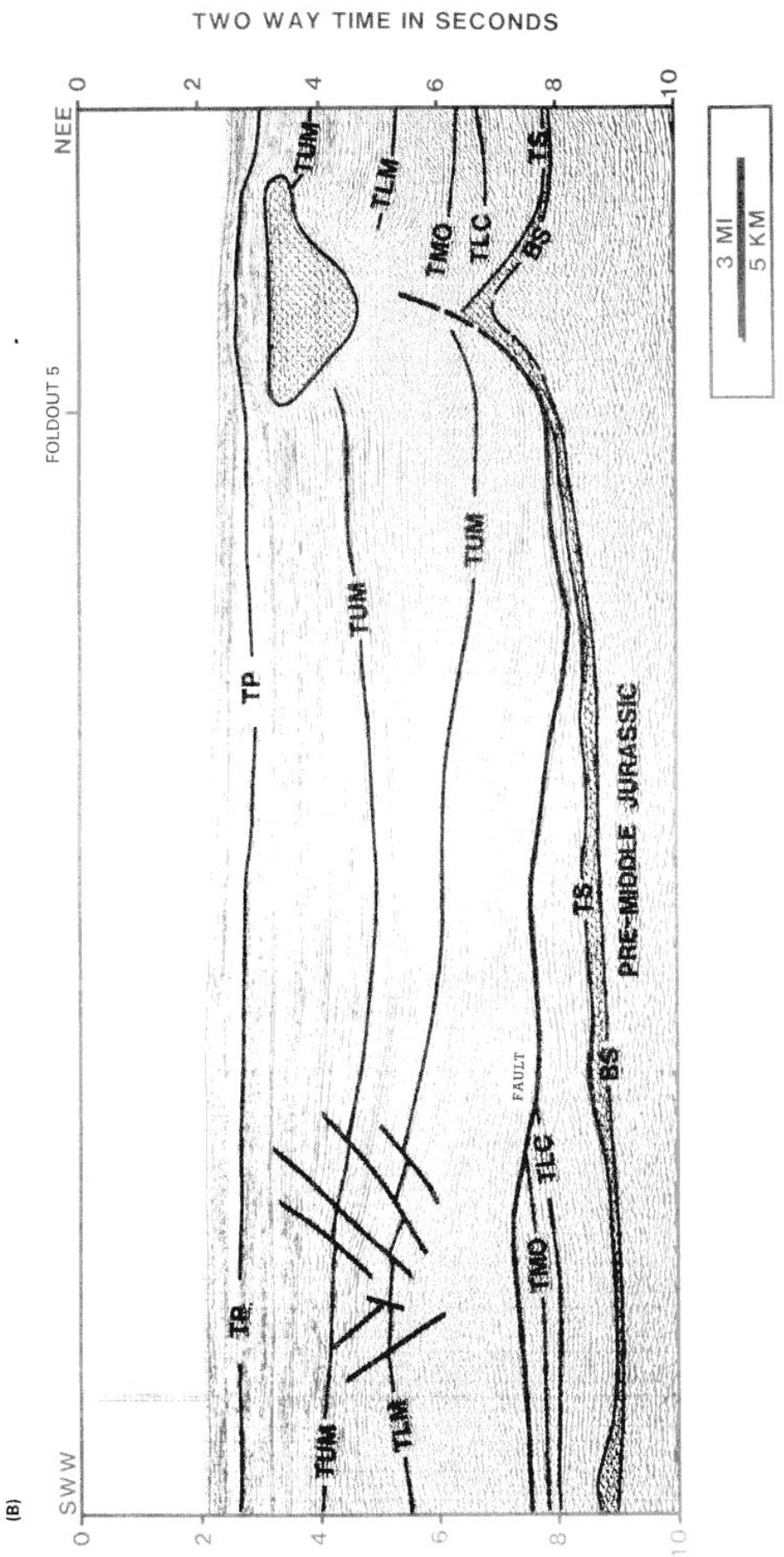

Figure 20 cont. **(B)** Interpreted seismic line in (A). Note that some salt moved along and over the fault plane into the present location while most of the salt moved down-slope forming the large salt sheet in *Foldout 5*

The detached allochthonous salt is illustrated by examples shown in *Foldouts 4* and *5* and *Figures 19–21*. The salt sheet in *Foldout 4* has many features in common with those of the salt tongue in *Figure 16* except that the salt sheet in *Foldout 4* is now completely separated from the feeder stock. Also, the salt sheet in *Foldout 4* has a larger areal extent than the tongue in *Figure 16 (Figure 12)*. It has spread about 80 km in the down-dip direction in an approximately 5 Ma period. The extent of allochthonous salt indicates that in a time interval, one of the factors that determines the spreading rate of a salt tongue or sheet is the amount of initial salt supply. *Foldout 4* shows a set of growth faults superimposed on an allochthonous salt sheet. A major down to the basin growth fault separates the salt sheet from its presumed original feeder stock. The down-slope withdrawal of salt from a feeder stock *(Figure 16)* accommodates the expansion of sediments in the down-thrown part of a major growth fault system *(Foldout 4)*. The work of Worrall and Snelson (1989) demonstrated that salt is the main factor that controls and accommodates the growth fault systems in the Gulf of Mexico. This example again shows that salt spreads preferentially in the down-slope direction. Once the salt tongue is separated from its feeder stock, the evolutionary stages of an allochthonous salt end and a new cycle of evolution begins.

The seismic examples of each evolutionary stage of allochthonous salt help to understand the allochthonous salt sheet shown in *Figure 3*. Part of *Figure 3* is shown in *Foldout 5* at a conventional scale. By comparing the allochthonous sheets in *Foldout 5* with *Foldout 4*, it is found that a similar set of down to the basin growth faults exist behind each of the detached salt sheets. The growth faults behind the salt sheets in each example sole out within allochthonous salt *(Foldouts 4* and *5)*. Both allochthonous salt masses were formed during the Miocene to Pliocene. In the example in *Foldout 5*, there is a down to the basin master growth fault, which soles out within the autochthonous salt. *Figure 20* shows a section perpendicular to *Foldout 5* across the master growth fault. Some salt moved up along and over the growth fault plane while most of the salt formed the large salt sheet.

An approximate reconstruction for the allochthonous salt in *Foldout 4* is attempted and shown in *Figure 21*. Moretti *et al.* (1990) present a computer-aided reconstruction of the same section. The reconstructed sections suggest evolutionary stages that are similar to those seen on the seismic examples in *Figures 13–16, 18, 19* and *Foldout 4*. A stage of salt concentration with salt pillows, swells and anticlines is shown in *Figure 21b*. Diapirism of the autochthonous salt stage started in the Late Oligocene–Early Miocene and is shown in *Figure 21c*. During Early Miocene, allochthonous salt tongues started to form. The allochthonous salt sheet extended greatly during the period of Middle and Upper Miocene *(Figure 21e)*. The allochthonous salt sheet was detached during the Pliocene when the sheet was separated by growth faults above the original feeder stock *(Figure 21c)*. The original feeder stock became a salt weld (Jackson and Cramez, 1989) after salt was squeezed upward.

Extension along the down to the basin master growth fault started after the Middle Cretaceous *(Figure 21b* and *c)* and continued into the Pliocene *(Figure 21e)*.

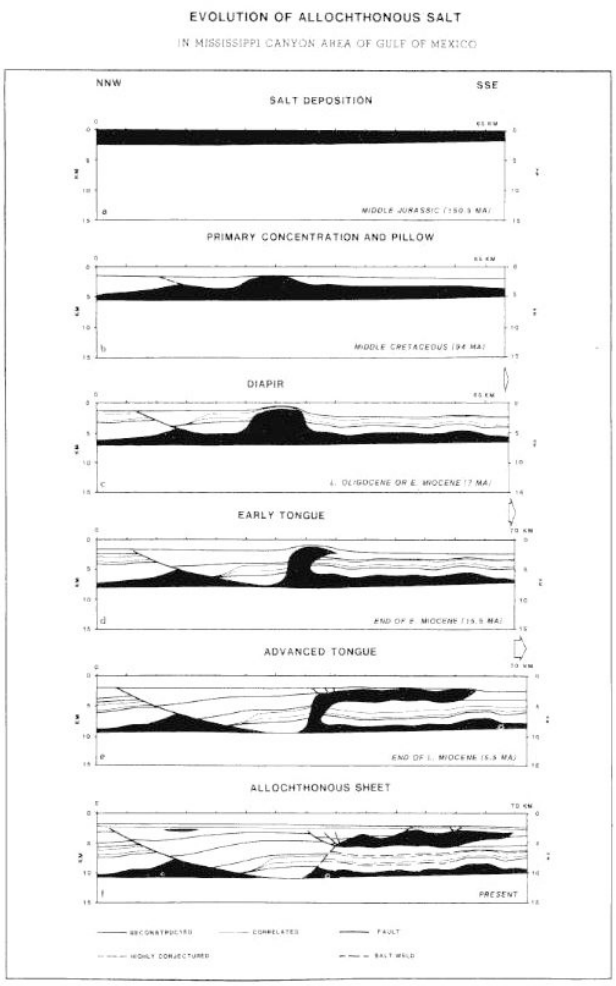

Figure 21 Hand-made reconstructions of the example in *Foldout 5*. The left end of the section is assumed to be fixed in space. The areas of the sediments except salt are kept constant in the reconstructions. Decompaction is not taken into account. Note that the area of salt (black) cannot be balanced within the plane of the page. A significant amount of salt moved out of the plane of the section. Salt is assumed to occupy all space between the base of autochthonous salt and the base of sediments overlying salt in the reconstructions. The exact reconstruction requires the knowledge of the amount of salt involved. The reconstructions show the evolutionary stages exemplified by seismic examples from the study area shown in *Figures 13–16, 18* and *Foldout 4*. The extension along the master down to the basin growth fault is compensated mainly by the withdrawal of salt from the original feeder stock and partly by basinward shortening as shown in *Figures 3* and *22* and *Foldout 6*. The partial extension possibly compensated by the basinward shortening is indicated by arrows. Major extensions occurred during the Miocene. The faults over the salt sheet sole out at the top of the allochthonous salt sheet

Major extension along the master growth fault occurred during the Miocene *(Figure 21c–d)*. The major extension was coeval with the shortening in the fold belt observed in the basinward direction of the salt sheet *(Figures 3* and *22* and *Foldouts 1* and *6)*. The extension was mainly compensated by the withdrawal of salt *(Figure 21e–f)* and partly by the down-slope shortening *(Figures 21b, 22* and *Foldout 6;* next section). However, to know the exact amount of extension compensated by each of the mechanisms requires a knowledge of the amount of salt involved in the process.

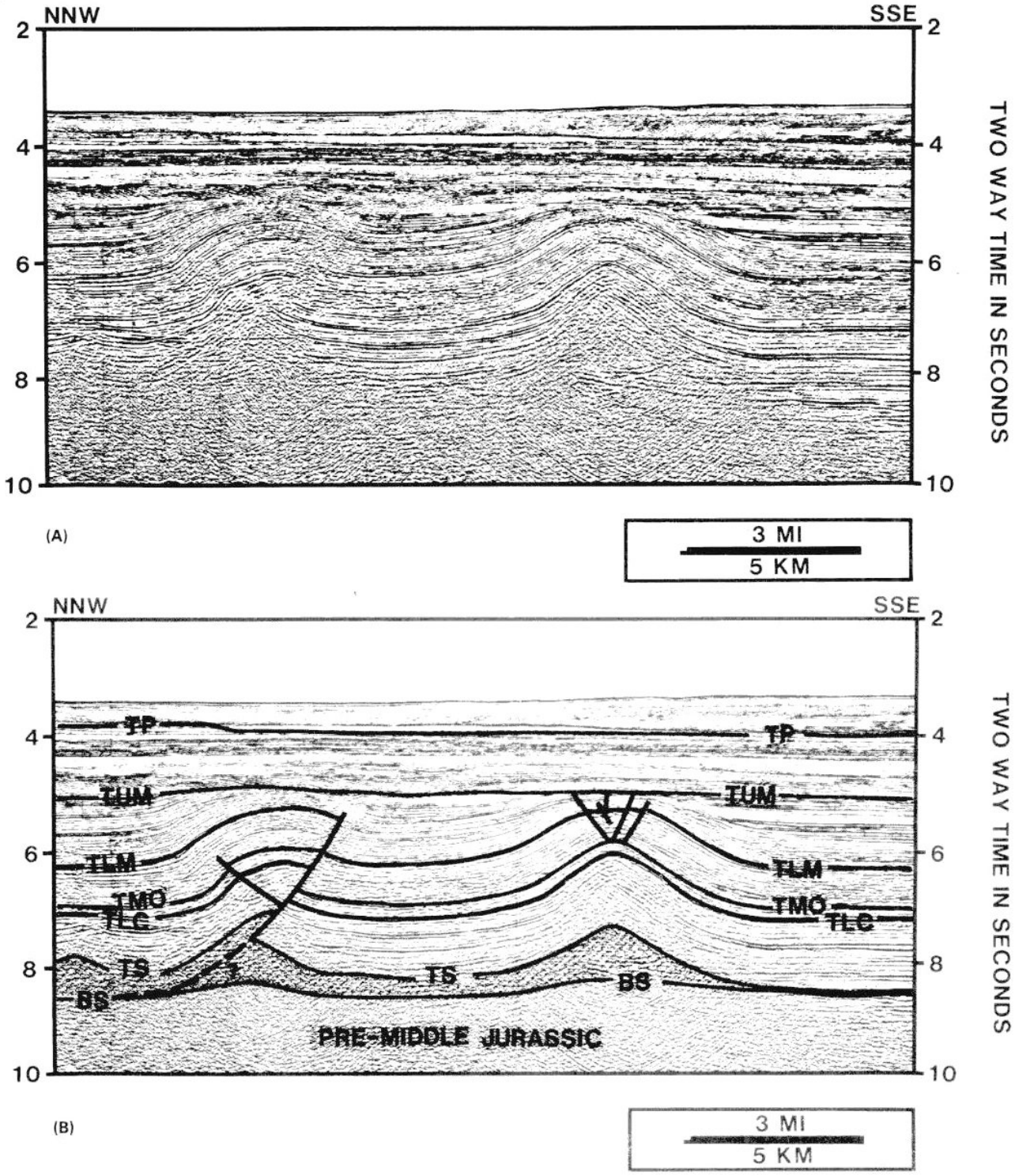

Figure 22 (A) Uninterpreted seismic example of a fold and thrust-faulted fold (courtesy of GECO). For location see *Figure 11*. **(B)** Interpreted example of (A). This example shows that the shortening started in about the Middle Miocene and ended by the end of the Upper Miocene. Jurassic Louann salt welts (Harrison and Bally, 1988) cored the fold and thrusted fold. Shortening ends at the basinward limit of the autochthonous salt

Mississippi Fan fold belt

A number of folds and thrusts forming the Mississippi Fan fold belt (Weimer and Buffler, 1989) are observed in the lower slope study area as illustrated by the regional seismic lines in *Figure 3* and *Foldout 1*. Additional examples of the Mississippi Fan fold belt are shown in *Figure 22* and *Foldout 6* (see *Figure 11* for locations). The fold belt is interpreted as cored by Jurassic Louann salt welts (Harrison and Bally, 1988). A major décollement of the fold belt is within the autochthonous salt. The thrust faults sole out within the autochthonous salt (*Figures 3* and *22* and *Foldouts 1* and *6*). The fold belt is mapped near the basinward limit of the autochthonous salt in *Figure 11*. Whether the fold belt extends northward and westward under the allochthonous salt to connect with the Perdido fold

belt of the western Gulf of Mexico is possible but unknown. Major shortening started in Late–Early Miocene *(Foldout 6)* and ceased before the end of the Late Miocene *(Figures 3* and *22* and *Foldouts 1* and *6)*. During the same period of active shortening, the depocentres of the Gulf of Mexico shifted into the study area; rates of sediment accumulation greatly increased *(Figures 3* and *22* and *Foldouts 3* and *6)*; and major relative upward growth and lateral spreading of salt occurred *(Figure 7)* followed by major extension along a down to the basin master growth fault *(Figures 3* and *21* and *Foldout 5)*. Autochthonous salt moved within the salt bed into the present fold belt as indicated by the salt welts and elevated sediments

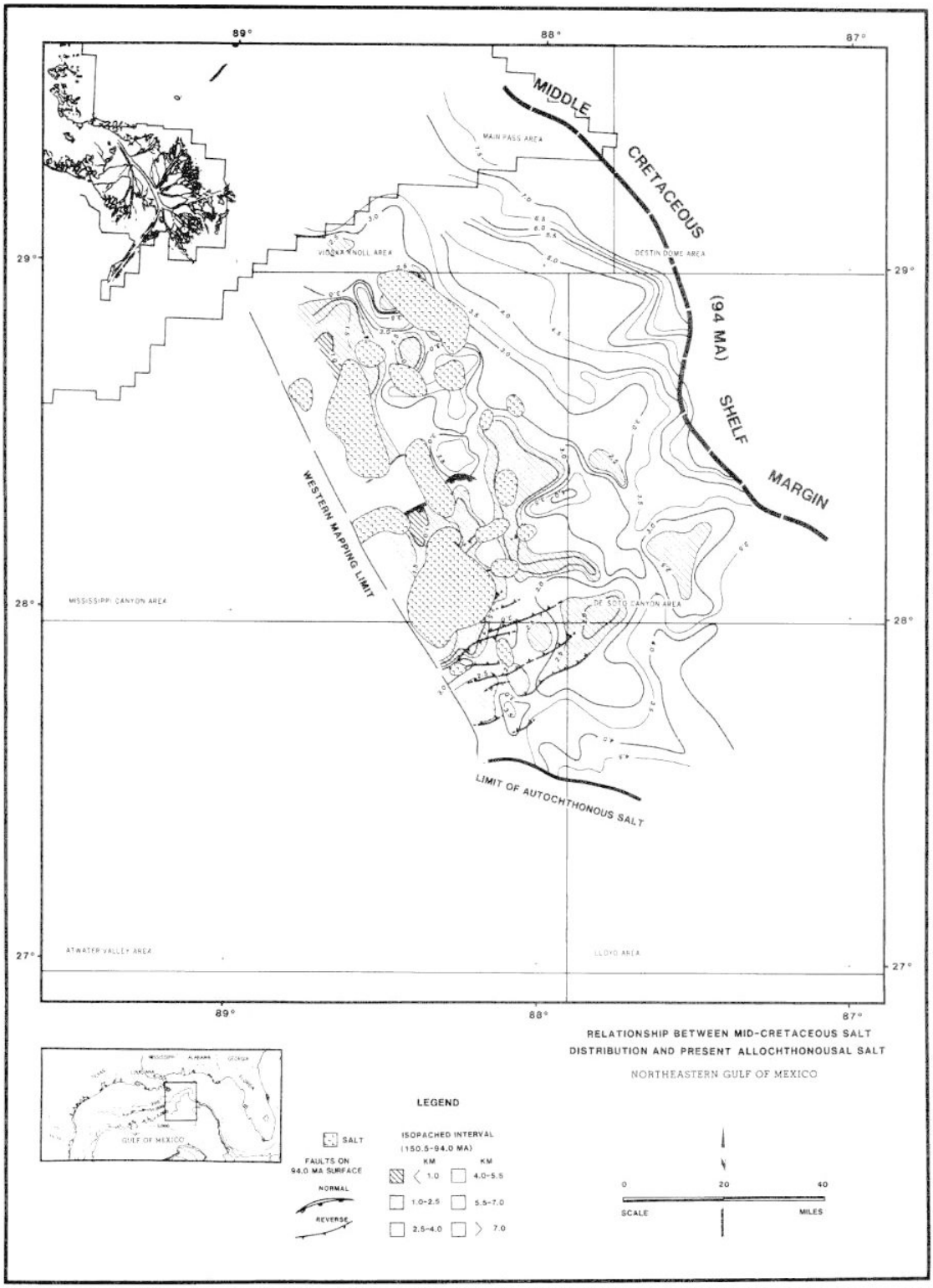

Figure 23 Map summarizing the relationship between the primary Mid-Cretaceous concentrated salt and the present day allochthonous salt tongues and sheets. It indicates that the allochthonous salt bodies sourced from the autochthonous salt concentrated by the Mid-Cretaceous. It also shows the positions of the basinward limit of the autochthonous salt and the fold and thrust belt

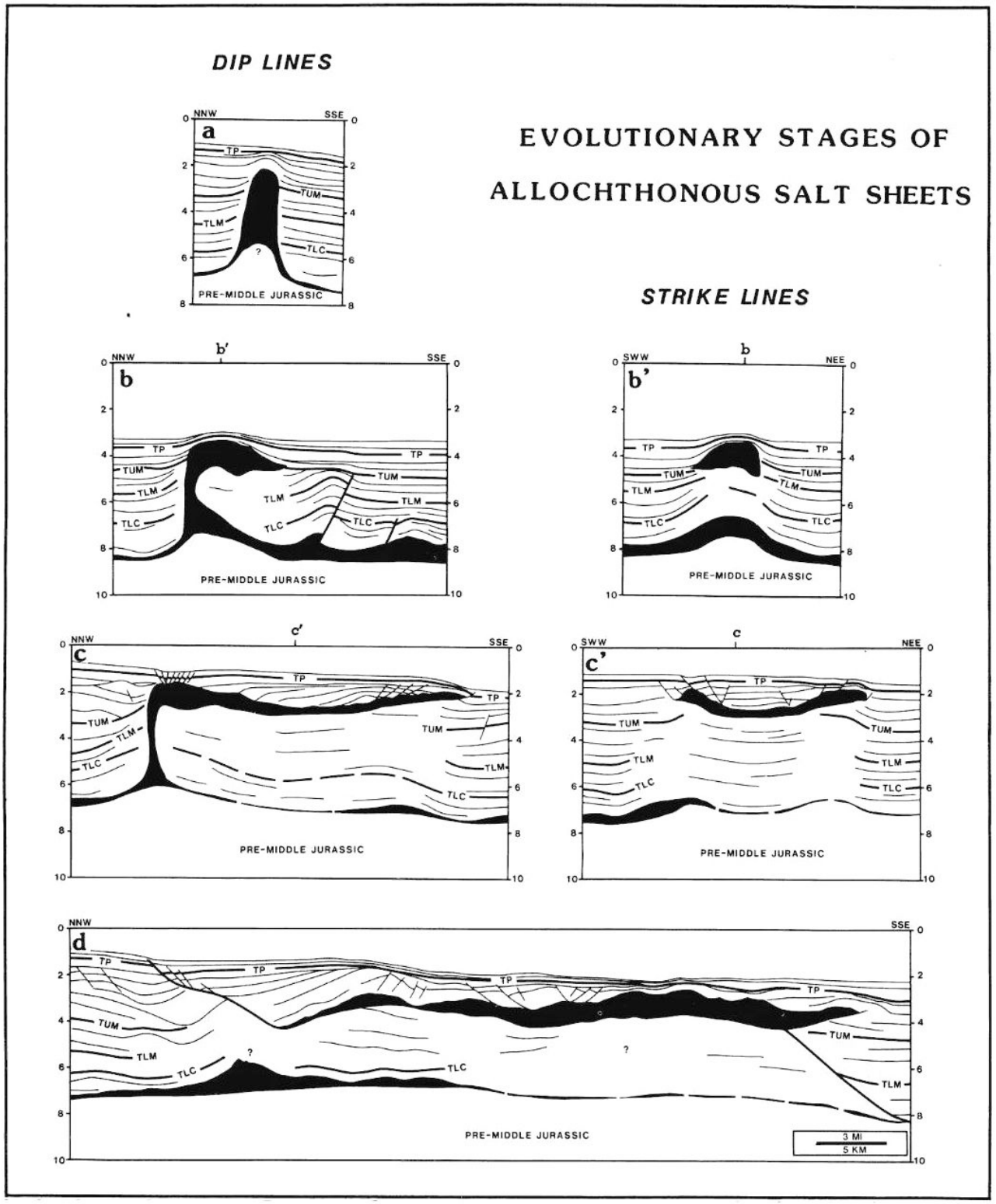

Figure 24 Summary of the evolutionary stages of an allochthonous salt sheet using line drawings of the seismic example shown previously (adapted from Wu *et al.*, 1989). (a) Autochthonous salt stage; (b), (b') allochthonous salt tongue; (c), (c') advanced allochthonous salt tongue; (d) detached allochthonous salt sheet

overlying salt *(Foldout 6)*. Extension along the master growth fault and diapirism of salt walls and domes have possibly contributed to the shortening in the Mississippi Fan fold belt. The Plio–Pleistocene growth fault system soling out at the allochthonous salt did not contribute to the formation of the fold belt because these faults were formed mostly after the shortening ceased. The extension along these growth faults is accommodated by salt withdrawal.

Summary

Our structural analysis uses a sequence stratigraphic frame of reference. A model for the evolution of allochthonous salt in north-eastern Gulf of Mexico is proposed. Excellent seismic examples along with

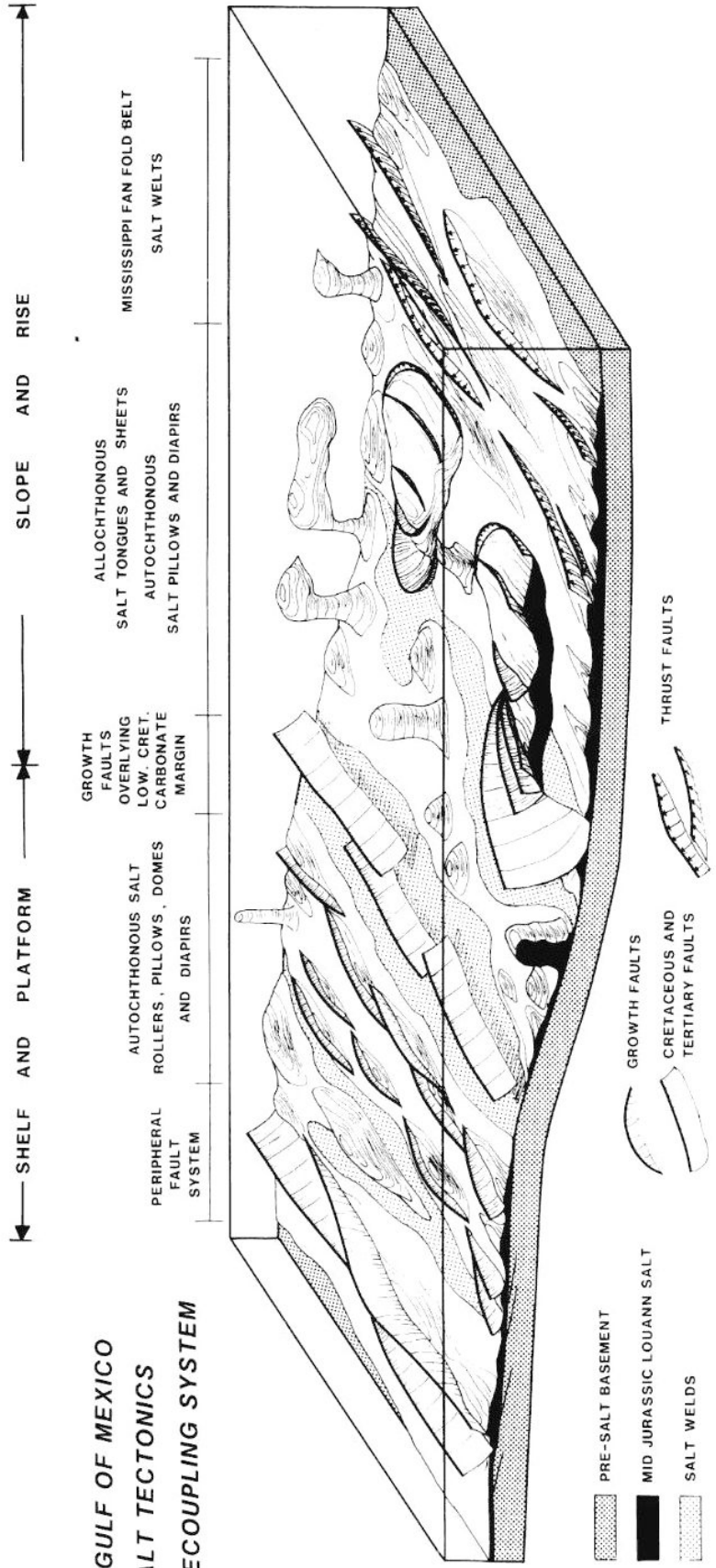

Figure 25 Schematic summary of salt tectonics and decoupling system in the north-eastern Gulf of Mexico. All the salt structures and the associated decoupling systems are shown by the presented seismic examples. See Jackson and Cramez (1989) for the definition of a weld and Harrison and Bally (1988) for the definition of a welt

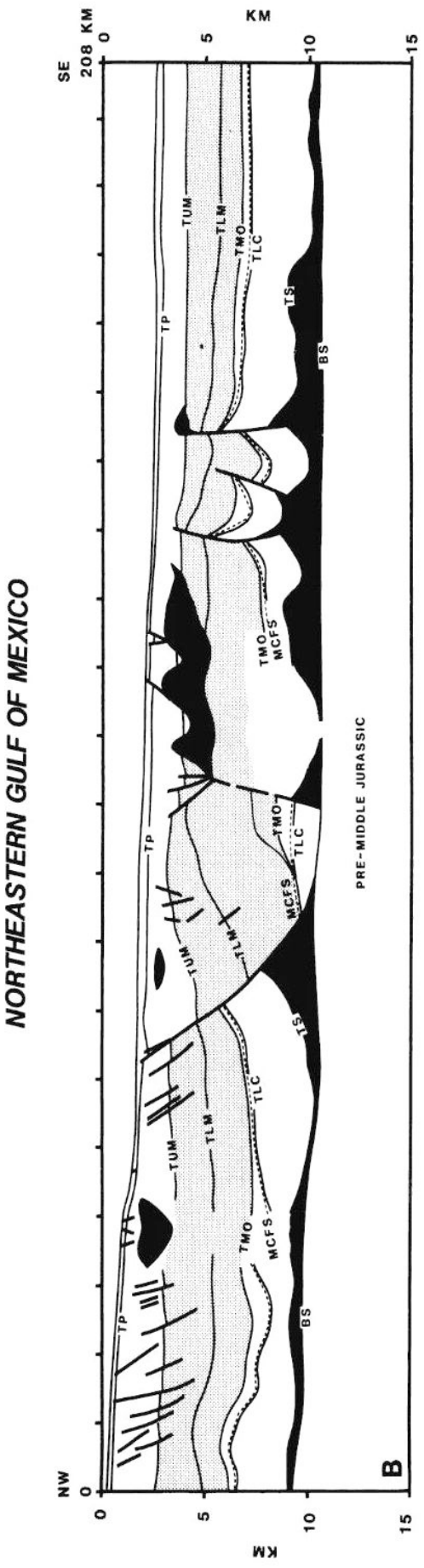

Figure 26 cont. **(B)** A depth section shown in *Foldout 5*. Vertical exaggeration = 3×. The basic architecture of the structural style is similar to that in (A) despite the scale difference. Both examples have a large allochthonous salt sheet, autochthonous salt and a fold belt. Growth faults soling out at the autochthonous and allochthonous salt exist in both sections. A set of faults developed on top of the allochthonous salt sheet. A bathymetric high developed in the leading part of the allochthonous salt sheet. The high was buried in (B) due to rapid Plio–Pleistocene deposition of Mississippi Fan while the high in the example from central Gulf of Mexico forms the Sigsbee Escarpment

reconstructions document each evolutionary stage of allochthonous salt and lead to the following conclusions:

(1) The base of Jurassic Louann Salt (undifferentiated from the base of the Werner Anhydrite underlying the Louann Salt) is a relatively smooth surface without major steps. Near the Florida Escarpment the surface is flexed, mainly due to Neogene–Pleistocene sediment loading. There is no major fault displacing the base of salt and separating the Florida Platform from continental slope of the Gulf of Mexico in the study area.

(2) As a consequence of sediment accumulation patterns in the north-eastern Gulf of Mexico, three major episodes of salt movement were documented. (a) Basinward salt movement towards the deep Gulf under lowstand and distal highstand sediment loads dominated in the slope area during 150.5–94 Ma leading to a primary salt concentration in large pillows and mounds *(Figures 7a–d* and *11)*. (b) An extended period of starved sedimentation during 94–30 Ma allowed these salt structures to stabilize *(Figure 7e)*.

(3) Rapid relative upward growth of salt structures occurred during the Early Miocene and Early Middle Miocene in response to rapid sediment accumulation. The formation of allochthonous salt tongues and sheets was due to dominant down-slope spreading and overthrusting of salt within the unconsolidated sediments during Middle Miocene to Plio–Pleistocene and was the consequence of continued rapid sediment accumulation (e.g. *Figure 7g–j*).

(4) Salt concentrations by 94 Ma had a great influence on the formation of allochthonous salt. Subsequently formed allochthonous salt tongues and sheets were fed from these early salt pillows and mounds *(Figure 23)*.

(5) The allochthonous salt presumably went through: (a) an autochthonous salt stage (in the form of rollers, swells, anticlines and domes and later in the form of diapiric salt walls and domes *(Figure 24a)*; (b) and allochthonous salt stage (in the form of tongues and sheets, e.g. *Figure 24b, b', c* and *c'*) and (c) the final detached allochthonous salt stage *(Foldout 5* and *Figure 24d)*. The presence of a slope and water softening of salt are two key factors that enhance the gravity spreading of salt. Sediment loads interact with spreading allochthonous salt tongues and salt sheets. Salt deforms as loaded by sediments and in turn fault patterns are closely related to the movements of salt *(Figure 17)*. A dynamic equilibrium is achieved between the sediment loading and salt deformation. The withdrawal of salt accommodates the expansion of growth faults above the feeder stock. Down to the basin growth fault systems separate the allochthonous salt from the original feeder stock. Salt weld is formed when the salt is completely displaced from its position.

(6) The salt structures and the associated decoupling system in the study area is schematically summarized in *Figure 25*. Autochthonous and allochthonous salt structures act as lower and upper decoupling levels, respectively. The lower level decoupling system is associated with the autochthonous salt. At this level, there are peripheral fault systems, salt rollers, down to the basin master growth faults and thrust faults. The higher decoupling level is associated with the allochthonous salt where various growth faults form (e.g. major down to the basin growth fault and

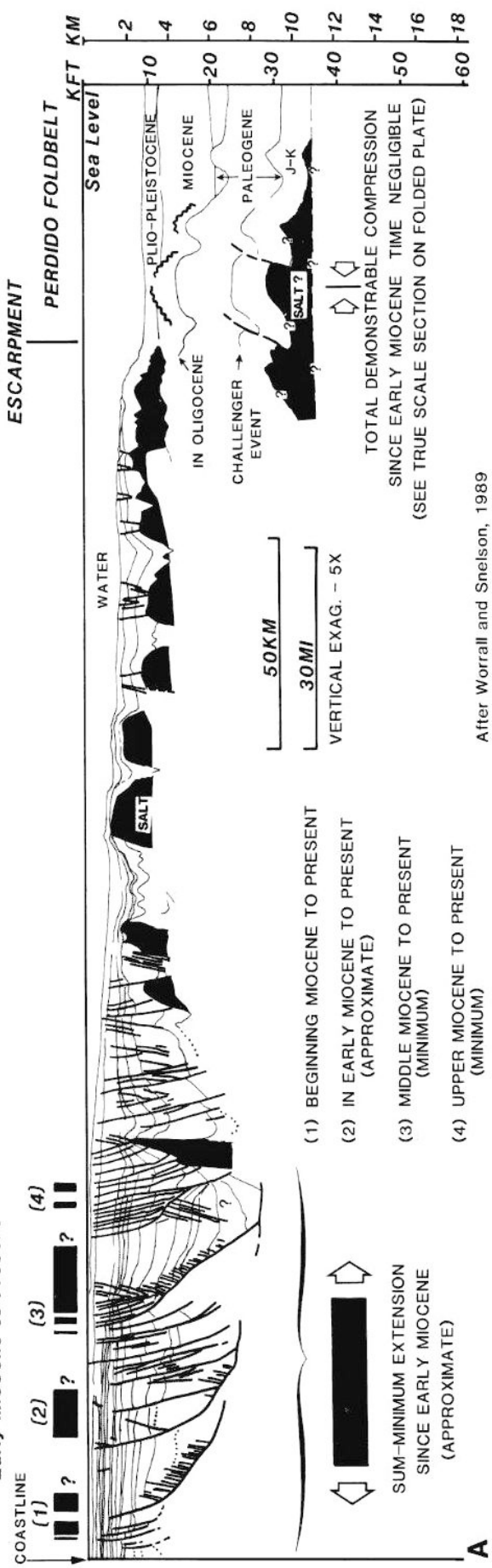

Figure 26 Comparison of a structural dip section from the central Gulf of Mexico (Redrawn after Worrall and Snelson, 1989) and a section from the Mississippi Canyon Area. **(A)** Structural cross-section, Texas coastline to the Sigsbee abyssal plain, showing minimum amounts of Miocene–Recent extension on Texas shelf (as measured by horizontal separation of correlated beds) compared to the amount of coeval shortening in the Perdido fold belt. Growth fault extension of this age is not accommodated in the Perdido foldbelt of mostly pre-Miocene age and must be accommodated in the salt rich slope region. Vertical exaggeration = 5×. For location see *Figure 1*. Part **(B)** is on the following page

counter-regional fault systems (Seni and Jackson, 1989)). The base of the allochthonous salt is an 'overthrust' surface. The extension along the down to the basin master growth fault system is mainly compensated by the withdrawal of salt from the feeder stock and partly by the shortening in the basinward direction.

Finally, a cross-section from the central Gulf of Mexico by Worrall and Snelson (1989) is compared with a section from the study area *(Figure 26)*. It shows that the structures associated with an allochthonous salt in the north-eastern Gulf of Mexico are analogous to the salt structures proposed by Worrall and Snelson (1989) in the central Gulf of Mexico. Because of the similar geological setting and the geometry of salt structures, the evolutionary model of the allochthonous salt presented in this paper may also apply to the evolutionary history of the salt structures associated with the Sigsbee Escarpment in the central Gulf of Mexico.

Acknowledgements

We are indebted to the generous support by Total Minatome Corporation, who provided all the data, facilities and financial support for this study. We thank Mr René Chappaz and Mr Henry Clemençon for their support. We appreciate the stimulating discussions held with our colleagues in the Offshore Exploration Department of Total Minatome Corporation. We thank M. P. A. Jackson for his constructive comments during this study. M. P. A. Jackson and Jake Hossack critically reviewed this paper. Their comments greatly improved the paper. We gratefully acknowledge the permission for publishing the seismic data from Geco Geophysical Company and Total Minatome Corporation.

References

Amery, G. B. (1969) Structure of Sigsbee scarp, Gulf of Mexico *AAPG Bull.* **53,** 2480–2482

Amery, G. B. (1978) Structure of continental slope, northern Gulf of Mexico. In: A. H. Bouma, G. T. Moore and J. M. Coleman (Eds.) *Framework, Facies, and Oil-Trapping Characteristics of the Upper Continental Margin: AAPG, Studies In Geology No. 7,* 141–153

Antoine, J. W. and Bryant, W. R. (1969) Distribution of salt and salt structures in Gulf of Mexico *AAPG Bull.* **53,** 2543–2550

Antoine, J. and Ewing, J. (1963) Seismic refraction measurements on the margins of the Gulf of Mexico *J. Geophys. Res.* **68,** 1975–1996

Bally, A. W. (1981) Thoughts on the tectonics of folded belts. In: K. R. McClay and N. J. Price (Eds.) *Thrust and Nappe Tectonics,* The Geological Society of London, London, 13–32

Barton, D. C. (1933) Mechanics of formation of salt domes with special reference to Gulf Coast salt domes of Texas and Louisiana *AAPG Bull.* **17,** 1025–1083

Bishop, R. S. (1978) Mechanism for emplacement of piercement diapirs *AAPG Bull.* **62,** 1561–1583

Buffler, R. T., Shaub, F. J., Watkins, J. S. and Worzel, J. L. (1978) Anatomy of the Mexican Ridges, southwestern Gulf of Mexico. In: J. S. Watkins, L. Montadert and P. W. Dickerson (Eds.) *Geological and Geophysical Investigations of Continental Margin: AAPG Memoir,* **29,** 319–327

Buffler, R. T., Worzel, J. L. and Watkins, J. S. (1978) Deformation and origin of the Sigsbee Scarp-lower continental slope, northern Gulf of Mexico. In: *Proceedings of 1978 Offshore Technology Conference* Vol 3, 1425–1433

Buffler, R. T. (1983) Structure of the Sigsbee Scarp, Gulf of Mexico. In: A. W. Bally (Ed.) *Seismic expression of structural styles — a picture and work atlas: AAPG Studies in Geology No. 15,* Vol 2, 2.3.2–50

Buffler, R. T. (1984) Early history and structure of the deep Gulf of Mexico Basin: Gulf Coast Section, SEPM Fifth Annual Foundation Research Conference, Austin, TX. USA, pp 31–34

de Jong, A. (1968) Stratigraphy of the Sigsbee Scarp from a reflection survey (abs.) *Society of Exploration Geophysicists Program, Fort Worth Mtg.,* 51

Ewing, M., Worzel, J. L., Ericson, D. B. and Heezen, B. C. (1955) Geophysical and geological investigations in the Gulf of Mexico, Part I *Geophysics* **20,** 1–18

Ewing, J., Antoine, J. and Ewing, M. (1960) Geophysical measurements in the western Caribbean Sea and in the Gulf of Mexico *J. Geophys. Res.* **65,** 4087–4103

Ewing, M., Antoine, J. (1966) New seismic data concerning sediments and diapiric structures in Sigsbee Deep and upper continental slope, Gulf of Mexico *AAPG Bull.* **50,** 479–504

Halbouty M. T. (1979) *Salt domes, Gulf region, United States and Mexico,* Gulf Publishing Co., Houston, TX, 561 pp.

Harrison, J. C. and Bally, A. W. (1988) Cross-sections of the Parry Islands fold belt on Melville Island, Canadian Arctic Islands: Implications for the timing and kinematic history of some thin-skinned décollement systems *Bull. Can. Petrol. Geol.* **36,** 311–332

Humphris, C. C., Jr (1978) *Salt movement on continental slope, northern Gulf of Mexico: AAPG Studies in Geology No. 7,* 69–85

Jackson, M. P. A. and Talbot, C. J. (1986) External shapes, strain rates, and dynamics of salt structures. *Geol. Soc. Am. Bull.* **97,** 305–323

Jackson, M. P. A., Talbot, C. J. and Cornelius, R. R. (1988) Centrifuge modelling of the effects of aggradation and progradation on syndepositional salt structures *Bureau of Economic Geology: Report of Investigations No. 173,* 93 pp.

Jackson, M. P. A. and Cramez, C. (1989) Seismic recognition of salt welds in salt tectonics regimes, extended and illustrated abstracts *Tenth Annual Research Conference Gulf Coast Section,* SEPM Foundation, Houston, TX, 66–71

Klitgord, K. D., Popenoe, P., Schouten, H. (1984) Florida: A Jurassic transform plate boundary. *J. Geophys. Res.* **89,** 7753–7772

Lehner, P. (1969) Salt tectonics and Pleistocene stratigraphy on continental slope of Northern Gulf of Mexico *AAPG Bull.* **53,** 2431–2479

Martin, R. G. (1978) Northern and eastern Gulf of Mexico continental margin: stratigraphy and structural framework. In: A. H. Bouma, G. T. Moore and J. M. Coleman (Eds.) *Framework, Facies and Oil-Trapping Characteristics of the Upper Continental Margin: AAPG, Studies In Geology No.7,* 21–42

Miller, E. T. and Ewing, M. (1956) Geomagnetic measurements in the Gulf of Mexico and in the vicinity of Caryn Peak *Geophysics* **21,** 406–432

Moore, G. T., Starke, G. W., Bonham, L. C. and Woodbury, H. D. (1978) Mississippi fan, Gulf of Mexico — physiography, stratigraphy, and sedimentational patterns. In: A. H. Bouma, G. T. Moore and J. M. Coleman (Eds.) *Framework, Facies, and Oil-Trapping Characteristics of the Upper Continental Margin: AAPG, Studies In Geology No.7* 155–191

Moretti, I., Wu, S. and Bally, A. W. (1990) Balanced Cross Section (LOCACE) to reconstruct allochthonous salt sheet, Offshore Louisiana *Mar. Petrol. Geol.,* **7,** 371–377

Nelson, T. N. and Fairchild, L. (1989) Emplacement and evolution of salt sills in the northern Gulf of Mexico *Houston Geol. Soc. Bull.,* September, 6–7

Nettleton, L. L. (1934) Fluid mechanics of salt domes *AAPG Bull.* **18,** 1175–1204

Nettleton, L. L. (1955) History of concepts of Gulf Coast salt-dome formation *AAPG Bull.* **39,** 2373–2383

NOAA, US Department of Commerce (1986) Regional Map of Gulf of Mexico, Scale 1:1000000

Odé, H. (1968) Review of mechanical properties of salt relating to salt dome genesis *Geol. Soc. Am. Spec. Paper 88,* 543–595

Ramberg, H. (1980) Diapirism and gravity collapse in the Scandinavian Caledonides *J. Geol. Soc. London* v. 137, 261–270

Ramberg, H. (1981) *Gravity, Deformation and the Earth's Crust,* 2nd Edition, Academic Press, London,452 pp.

Sannemann, D. (1968) Salt-stock families in northeastern Germany. In: J. Braunstein and G. D. O'Brien (Eds.) *Diapirism and Diapirs: AAPG Memoir* **8,** 261–270

Seni, S. J. and Jackson, M. P. A. (1989) Counter-regional growth faults and salt sheet emplacement, northern Gulf of Mexico, extended and illustrated abstracts *Tenth Annual Research Conference Gulf Coast Section,* SEPM Foundation, Houston, TX, 116–121

Talbot, C. J. and Rogers, E. A. (1980) Seasonal movements in a salt glacier in Iran *Science* **208,** 395–397

Talbot, C. J. and Jarvis, R. J. (1984) Age, budget and dynamics of an active salt extrusion in Iran *J. Struc. Geol.* **6,** 521–533

Talbot, C. J. and Jackson, M. P. A. (1987a) Salt tectonics *Sci. Am.* **257,** 70–79

Talbot, C. J. and Jackson, M. P. A. (1987b) Internal kinematics of salt diapirs *AAPG Bull.* **7,** 1068–1093

Talwani, M. and Ewing, M. (1966) A continuous gravity profile over the Sigsbee Knolls *J. Geophys. Res.* **71,** 4434–4438

Trusheim, F. (1960) Mechanism of salt migration in northern Germany *AAPG Bull.* **44,** 1519–1540

Tyrrell, W. W., Jr and Scott, R. W. (1988) Early Cretaceous shelf margins, Vernon Parish, Louisiana. In: A. W. Bally (Ed.) *Atlas of Seismic Stratigraphy: AAPG Studies in Geology, No.27* Vol 3, 11–16

Watkins, J. S., Ladd, J. W., Buffler, R. T., Shaub, F., Houston, M. H. and Worzel, J. L. (1978) Occurrence and evolution of salt in deep Gulf of Mexico. In: A. H. Bouma, G. T. Moore and J.M. Coleman (Eds.) *Framework, Facies and Oil-Trapping Characteristics of the Upper Continental Margin: AAPG, Studies in Geology No.7,* 43–65

Weimer, P. (1989) Sequence stratigraphy of the Mississippi Fan (Plio-Pleistocene) Gulf of Mexico *Geo-Mar. Lett.* **9,** 185–272

Weimer, P. and Buffler, R. T. (1989) Structural geology of the Mississippi Fan foldbelt, deep Gulf of Mexico, extended and illustrated abstracts *Tenth Annual Research Conference Gulf Coast Section* SEPM Foundation, Houston, TX, 146–147

West, D. B. (1989) Model for salt deformation on deep margin of central Gulf of Mexico basin *AAPG Bull.* **73,** 1473–1482

Wilhelm, O. and Ewing, M. (1972) Geology and history of the Gulf of Mexico *Geol. Soc. Am. Bull.* **83,** 575–600

Worrall, D. M. and Snelson, S. (1989) Evolution of the northern Gulf of Mexico, with emphasis on Cenozoic growth faulting and the role of salt. In: A. W. Bally and A. R. Palmer (Eds.) *Geological Society of America Centennial Special Volume, The Geology of North America,* GSA, Washington, 97–138

Wu, S., Cramez, C., Bally, A. W., Vail, P. R. (1989) Evolution of allochthonous salt in Mississippi Canyon Area, extended and illustrated abstracts *Tenth Annual Research Conference Gulf Coast Section* SEPM Foundation, Houston, TX, 161–165

Wu, S., Vail, P. R. and Cramez, C. (1990) Allochthonous salt, structure and stratigraphy of the north-eastern Gulf of Mexico. Part I: Stratigraphy *Mar. Petrol. Geol.* **7,** 318–333